

# Inference in generative models using the Wasserstein distance

Esben Bernton <sup>\*</sup>, Pierre E. Jacob<sup>\*</sup>, Mathieu Gerber<sup>†</sup>, Christian P. Robert<sup>‡</sup>

## Abstract

In purely generative models, one can simulate data given parameters but not necessarily evaluate the likelihood. We use Wasserstein distances between empirical distributions of observed data and empirical distributions of synthetic data drawn from such models to estimate their parameters. Previous interest in the Wasserstein distance for statistical inference has been mainly theoretical, due to computational limitations. Thanks to recent advances in numerical transport, the computation of these distances has become feasible, up to controllable approximation errors. We leverage these advances to propose point estimators and quasi-Bayesian distributions for parameter inference, first for independent data. For dependent data, we extend the approach by using delay reconstruction and residual reconstruction techniques. For large data sets, we propose an alternative distance using the Hilbert space-filling curve, which computation scales as  $n \log n$  where  $n$  is the size of the data. We provide a theoretical study of the proposed estimators, and adaptive Monte Carlo algorithms to approximate them. The approach is illustrated on four examples: a quantile g-and-k distribution, a toggle switch model from systems biology, a Lotka-Volterra model for plankton population sizes and a Lévy-driven stochastic volatility model.

## 1 Introduction

The likelihood function plays a central role in statistics, and arguably provides all the relevant information for inference (Berger and Wolpert, 1988). However, for many models of interest, the likelihood cannot be evaluated, often because it involves an intractable integral over latent variables. It might be possible to generate synthetic data sets given parameters, in which case the model is said to be generative. This article is about statistical inference for generative models.

To perform inference in generative models, a popular approach consists in replacing the likelihood by an approximation and aiming for either point estimators (Diggle and Gratton, 1984; Wood, 2010), or quasi-posterior distributions, leading to Approximate Bayesian Computation (ABC) (Beaumont et al., 2002). Other approaches include indirect inference (Gouriéroux et al., 1993) and the method of simulated moments (McFadden, 1989); insightful reviews can be found in Marin et al. (2012); Forneron and Ng (2015), and connections with generative adversarial networks in Mohamed and Lakshminarayanan (2016). These approaches typically rely on appropriate choices of summary statistics or auxiliary models.

In the spirit of minimum distance estimation (Wolfowitz, 1957; Basu et al., 2011), we propose new inferential methods for generative models, bypassing the choice of summary statistics altogether. Relatively few approaches have been proposed to bypass that choice (Park et al., 2016; Zuluaga et al., 2015; Prangle

---

<sup>\*</sup>Department of Statistics, Harvard University, USA, ebernton@g.harvard.edu and pjacob@g.harvard.edu

<sup>†</sup>School of Mathematics, University of Bristol, UK

<sup>‡</sup>CEREMADE, Université Paris-Dauphine, PSL Research University, France, and Department of Statistics, University of Warwick, UK

et al., 2016). We argue that the Wasserstein distance, also called the Gini, Mallows, or Kantorovich distance, provides a compelling tool to compare empirical distributions generated from the model with the empirical distribution of the observations. This translates to parameter inference via an optimization program on the parameter space, or via a sampling problem in a Bayesian setting, very similar to ABC. The Wasserstein distance leads to estimators than can be theoretically studied, as initiated in Bassetti et al. (2006); Bassetti and Regazzini (2006). We extend their results on consistency, rates of convergence and asymptotic distributions. Wasserstein distances are defined via an optimal transport program and their calculation is greatly facilitated by recent advances in numerical transport (Cuturi, 2013; Cuturi and Doucet, 2014; Genevay et al., 2016). Recently, Montavon et al. (2016) have used these advances to perform parameter inference in models for which the derivative of the log-likelihood can be computed, which is not the case for purely generative models.

Furthermore, we consider computationally advantageous alternatives to the Wasserstein distance, using the Hilbert space-filling curve (Sagan, 1994; Gerber and Chopin, 2015b), which provides an order of magnitude speed-up for large data sets. We extend the methodology to dependent data using delay reconstruction and residual reconstruction. Throughout the article, we work under model misspecification unless otherwise stated: we do not assume that the observations are realizations of our model distributions.

Minimum distance estimation with the Wasserstein distance provides a generic inference scheme for generative models. Our contributions are: 1) new algorithms for parameter inference in the setting of purely generative models, without using summary statistics, 2) extension of the proposed method to dependent data, 3) a theoretical study of the asymptotic behavior of the proposed estimators. This article draws novel connections between the areas of minimum distance estimation, approximate Bayesian computation, numerical transport, space-filling curves and delay reconstruction of dynamical systems.

Section 2 introduces the main ideas and illustrates them on simple examples. Section 3 discusses extensions to dependent data. Section 4 presents some theoretical contributions on minimum Wasserstein estimation and associated quasi-posterior distributions. Section 5 discusses computational aspects, including distance computation, optimization techniques and sampling algorithms. Section 6 contains numerical experiments on two models with independent data, a quantile g-and-k distribution and a toggle switch model from systems biology, and two state space models, a Lotka-Volterra model and a Lévy-driven stochastic volatility model. The code is available on GitHub at [github.com/pierrejacob/winference](https://github.com/pierrejacob/winference). Proofs can be found in the supplementary materials on the webpage of the second author.

## 2 Minimum distance inference for generative models

### 2.1 Generative models and notation

We work on a probability space  $(\Omega, \mathcal{F}, \mathbb{P})$  with associated expectation operator  $\mathbb{E}$ . The data take values in  $\mathcal{Y}$ , a subset of  $\mathbb{R}^{d_y}$  for  $d_y \in \mathbb{N}$ . We observe  $n \in \mathbb{N}$  data points  $y_1, \dots, y_n$ , also denoted  $y_{1:n}$ . We denote by  $\mathcal{P}(\mathcal{X})$  the set of probability measures on some space  $\mathcal{X}$ . We assume that the data are distributed according to  $\mu_{\star}^{(n)} \in \mathcal{P}(\mathcal{Y}^n)$ . For independent and identically distributed (i.i.d.) data,  $\mu_{\star}^{(n)}$  is the  $n$ -product of a marginal distribution  $\mu_{\star}$  in  $\mathcal{P}(\mathcal{Y})$ . The empirical distribution of the data  $y_{1:n}$  is  $\hat{\mu}_n = n^{-1} \sum_{i=1}^n \delta_{y_i}$ , where  $\delta_y$  denotes the Dirac distribution with point mass on  $y \in \mathcal{Y}$ .

We consider a model to be a collection of distributions on  $\mathcal{Y}$ , denoted by  $\mathcal{M} = \{\mu_{\theta} : \theta \in \mathcal{H}\} \subset \mathcal{P}(\mathcal{Y})$ , where  $\mathcal{H}$  is the parameter space, endowed with a distance  $\rho_{\mathcal{H}}$  and assumed to be a subset of  $\mathbb{R}^{d_{\theta}}$  for  $d_{\theta} \in \mathbb{N}$ . For the moment, we assume that we generate synthetic data i.i.d. from  $\mu_{\theta}$ , with joint denoted  $\mu_{\theta}^{(n)}$ , and

elaborate on extensions to non-i.i.d. data in Section 3. A model is well-specified if there exists  $\theta_* \in \mathcal{H}$  such that  $\mu_* = \mu_{\theta_*}$ ; otherwise it is misspecified. We say that it is identifiable if  $\theta = \theta'$  is implied by  $\mu_\theta = \mu_{\theta'}$ . We consider the context of purely generative models, where it is possible to generate observations  $z_{1:n}$  from  $\mu_\theta^{(n)}$ , for all  $\theta \in \mathcal{H}$ , but it is not possible to evaluate the associated likelihood.

## 2.2 Minimum distance estimation

Minimum distance estimation refers to the idea of minimizing, over the parameter  $\theta \in \mathcal{H}$ , a distance between the empirical distribution  $\hat{\mu}_n$  and the model distribution  $\mu_\theta$  (Wolfowitz, 1957; Basu et al., 2011). In these broad terms, it encompasses the spirit of various statistical paradigms: for instance, the maximum likelihood approach asymptotically minimizes the Kullback-Leibler (KL) divergence between  $\mu_*$  and  $\mu_\theta$ , defined as  $\text{KL}(\mu_*|\mu_\theta) = \int \log(d\mu_*/d\mu_\theta) d\mu_*$ . The empirical likelihood method minimizes a KL divergence between the empirical distribution and a model supported on the observed data under moment conditions (Owen, 2001). Any choice of distance, or pseudo-distance measuring the similarity between two distributions, yields an associated minimum distance estimator. Denoting by  $\mathfrak{D}$  a distance or divergence on  $\mathcal{P}(\mathcal{Y})$ , the associated minimum distance estimator can be defined as

$$\hat{\theta}_n = \operatorname{arginf}_{\theta \in \mathcal{H}} \mathfrak{D}(\hat{\mu}_n, \mu_\theta). \quad (1)$$

This raises multiple statistical and computational questions. First, the distance  $\mathfrak{D}$  needs to be a meaningful notion of similarity between distributions, including empirical distributions with unequal discrete supports. This precludes some distances, such as the total variation distance. Statistically, the estimator  $\hat{\theta}_n$  should preferably satisfy some properties, under conditions on  $\mathfrak{D}$ , the data-generating distribution  $\mu_*$  and the model  $\mathcal{M}$ . Particularly important properties include existence and measurability of  $\hat{\theta}_n$ , uniqueness and consistency when  $n \rightarrow \infty$ . Further interesting aspects include rates of convergence, asymptotic distributions, and robustness to outliers.

The distance  $\mathfrak{D}$  needs to be computable, at least up to a certain accuracy, so that we can realistically envision the above optimization program. Since the data might be multivariate ( $d_y > 1$ ), some familiar distances such as the Kolmogorov–Smirnov distance might prove computationally inconvenient. Finally, in the context of purely generative models, it will often be more convenient to consider the alternative estimator

$$\hat{\theta}_{n,m} = \operatorname{arginf}_{\theta \in \mathcal{H}} \mathbb{E} [\mathfrak{D}(\hat{\mu}_n, \hat{\mu}_{\theta,m})]. \quad (2)$$

where  $\hat{\mu}_{\theta,m}$  is the empirical distribution of a sample  $z_{1:m} \sim \mu_\theta^{(m)}$ , and the expectation is with respect to the randomness of that sample. When  $n$  is fixed and  $m$  is large, or when  $n = m$  and  $n$  is large, we expect the expectation to be close to  $\mathfrak{D}(\hat{\mu}_n, \mu_\theta)$ , and the two estimators to have similar properties.

## 2.3 Wasserstein distance and point estimators

Factoring in the above considerations, we consider the Wasserstein distance for  $\mathfrak{D}$ . Let  $\rho$  be a distance on  $\mathcal{Y}$ . Let  $\mathcal{P}_p(\mathcal{Y})$  with  $p \geq 1$  be the subset of  $\mathcal{P}(\mathcal{Y})$  of distributions with finite  $p$ -th moment, that is

$$\mathcal{P}_p(\mathcal{Y}) = \left\{ \mu \in \mathcal{P}(\mathcal{Y}) : \exists y_0 \in \mathcal{Y} \text{ st. } \int_{\mathcal{Y}} \rho(y, y_0)^p d\mu(y) < \infty \right\}.$$

This space is referred to as the  $p$ -Wasserstein space of probability distributions on  $\mathcal{Y}$  (Villani, 2008).

**Definition 2.1.** The  $p$ -Wasserstein distance is a (finite) metric on  $\mathcal{P}_p(\mathcal{Y})$  defined by

$$\mathfrak{W}_p(\mu, \nu) = \left( \inf_{\gamma \in \Gamma(\mu, \nu)} \int_{\mathcal{Y} \times \mathcal{Y}} \rho(x, y)^p d\gamma(x, y) \right)^{1/p}, \quad (3)$$

where  $\Gamma(\mu, \nu)$  is the set of all Radon probability measures on  $\mathcal{Y} \times \mathcal{Y}$  with marginals  $\mu$  and  $\nu$  respectively.

This distance can be traced back to Gini (1914) and was developed in Kantorovich (1942); Wasserstein (1969), see notes in Chapter 6 of Villani (2008). We write  $\mathfrak{W}_p(y_{1:n}, z_{1:m})$  for  $\mathfrak{W}_p(\hat{\mu}_n, \hat{\nu}_m)$ , where  $\hat{\mu}_n$  and  $\hat{\nu}_m$  stand for the empirical distributions  $n^{-1} \sum_{i=1}^n \delta_{y_i}$  and  $m^{-1} \sum_{i=1}^m \delta_{z_i}$ .

An important special case is where  $\mathcal{Y} = \mathbb{R}$  and  $\rho(x, y) = |x - y|$ . Under this setup, the  $p$ -Wasserstein distance reduces to

$$\mathfrak{W}_p(\mu, \nu) = \left( \int_0^1 |F_\mu^{-1}(s) - F_\nu^{-1}(s)|^p ds \right)^{1/p} \quad (4)$$

where  $F_\mu(t) = \mu(-\infty, t]$  and  $F_\mu^{-1}(s) = \inf\{x \in \mathbb{R} : s \leq F_\mu(t)\}$ ; see Proposition 2.17 in Santambrogio (2015). Therefore, the Wasserstein distance for empirical distributions on  $\mathbb{R}$  takes the simple form

$$\mathfrak{W}_p(y_{1:n}, z_{1:n}) = \left( \frac{1}{n} \sum_{i=1}^n |y_{(i)} - z_{(i)}|^p \right)^{1/p}, \quad (5)$$

where  $y_{(i)}$  and  $z_{(i)}$  denote the  $i$ -th order statistics of the samples. The cost of computing that distance is thus in  $n \log n$ . In the multivariate case ( $d_y > 1$ ), there is no such simple representation and the cost of computing the Wasserstein distance is much larger, as discussed in Section 5.1. We will then rely on fast distance approximations discussed in Sections 5.1-5.2.

By plugging  $\mathfrak{W}_p$  in place of  $\mathfrak{D}$  in Eqs. (1) and (2), we obtain the minimum Wasserstein estimator (MWE) and minimum expected Wasserstein estimator (MEWE) of order  $p$ , denoted  $\hat{\theta}_n$  and  $\hat{\theta}_{n,m}$  respectively. Some properties of the MWE have been studied in Bassetti et al. (2006), for well-specified models and i.i.d. data; we propose new results in Section 4. Intuitively, under some conditions we can expect  $\hat{\mu}_n$  to converge to  $\mu_*$ , in the sense that  $\mathfrak{W}_p(\hat{\mu}_n, \mu_*) \rightarrow 0$ . Consequently, the minimum of  $\theta \mapsto \mathfrak{W}_p(\hat{\mu}_n, \mu_\theta)$  might converge to the minimum of  $\theta \mapsto \mathfrak{W}_p(\mu_*, \mu_\theta)$ , denoted by  $\theta_*$ , assuming its existence and unicity. In the well-specified case,  $\theta_*$  coincides with the data-generating parameter. In the misspecified case,  $\theta_*$  is typically different from the limit of the maximum likelihood estimator (MLE), which is the minimizer of  $\text{KL}(\mu_* | \mu_\theta)$ . While the KL divergence is a central notion in information theory, and is defined irrespective of the metric on the data space  $\mathcal{Y}$ , the Wasserstein distance is related to optimal transport theory, depends on the choice of metric  $\rho$ , and is a proper distance between probability measures. Both lead to principled statistical procedures, but we argue in this article that the MWE has computational advantages over the MLE in the context of generative models.

**Example 2.1.** Let  $\mu_* = \text{Gamma}(10, 5)$  (parametrized by shape and rate) and  $\mathcal{M} = \{N(\mu, \sigma^2) : \mu \in \mathbb{R}, \sigma > 0\}$ . Figure 1 compares the sampling distributions of the MLE and of the MEWE of order 1, over  $M = 1,000$  experiments. The MEWE converges at the same  $\sqrt{n}$  rate as the MLE, albeit to a distribution that is centered at a different location and with somewhat higher variance. For the MEWE, we have used  $m = 10^4$  and defer to Section 5.3 for computational aspects.

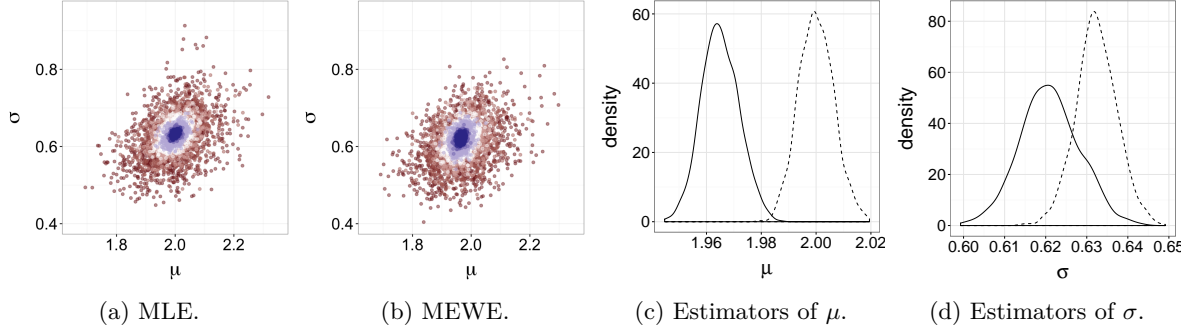


Figure 1: Figure 1a and 1b show the sampling distributions of the MLE and MEWE of order 1 respectively, as  $n$  ranges from 50 to  $10^4$  (colors from red to white to blue). Figure 1c and 1d show the marginal densities of the estimators of  $\mu$  and  $\sigma$  respectively, for  $n = 10^4$ ; the MLEs are shown in dashed lines and the MEWE in full lines. These plots correspond to Example 2.1.

**Example 2.2.** Let  $\mu_*$  be Cauchy with median zero and scale one, and consider the model  $\mathcal{M} = \{N(\mu, \sigma^2) : \mu \in \mathbb{R}, \sigma > 0\}$ . Neither the MLE nor the MEWE of order  $p \geq 2$  converges in this setting. We explore the behavior of the MEWE of order 1, over  $M = 1,000$  repeated experiments. Figure 2 shows its sampling distributions, for  $n$  ranging from 50 to  $10^4$ . The marginal distribution of the estimator of  $\mu$  concentrates around 0, the median of  $\mu_*$ . The marginal distribution of the estimator of  $\sigma$  also concentrates, around a value between 2 and 2.5. The concentration occurs at rate  $\sqrt{n}$ , as shown by the marginal densities of the rescaled estimators of  $\mu$  in Figure 2b.

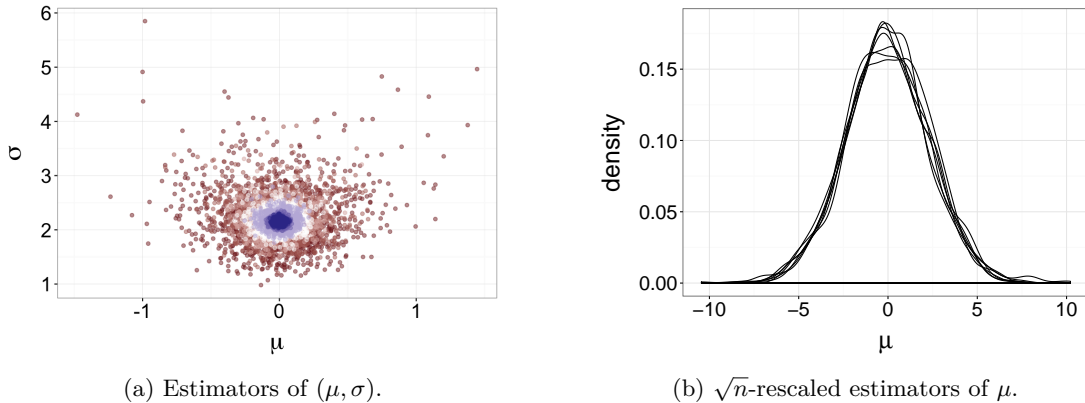


Figure 2: Sampling distributions of MEWE as  $n$  ranges from 50 to  $10^4$  (colors from red to white to blue, left). The marginals of MEWE of  $\mu$ , rescaled by  $\sqrt{n}$ , are shown on the right. These plots correspond to Example 2.2.

Example 2.2 illustrates the robustness of the MEWE of order 1 compared to the MLE. Bassetti and Regazzini (2006) study the influence functions for the MWE of order 1 in a location model, and show that it is bounded. Other references on robustness in minimum distance estimation include Parr and Schucany (1980).

## 2.4 Probabilistic inference and approximate Bayesian computation

We introduce a Bayesian framework, which provides a probabilistic alternative to point estimators. This framework allows close connections with ABC, and is in fact equivalent to ABC in some special cases. The

framework fruitfully leads to Monte Carlo methods, that are also useful for point estimation (similarly to [Wood, 2010](#); [Rubio et al., 2013](#)). We introduce a prior distribution  $\pi$  on the parameter  $\theta$ . The following algorithm is referred to as the Wasserstein rejection sampler.

1. Draw a parameter  $\theta$  from the prior distribution  $\pi$ . Draw a synthetic dataset  $z_{1:n} \sim \mu_\theta^{(n)}$ .
2. If the distance  $\mathfrak{W}_p(y_{1:n}, z_{1:n})$  is less than a threshold  $\varepsilon > 0$ , keep the parameter  $\theta$ , otherwise reject it.

By comparison, ABC methods use a distance between summary statistics,  $\eta(y_{1:n})$  and  $\eta(z_{1:n})$ , where  $\eta : \mathcal{Y}^n \rightarrow \mathbb{R}^{d_\eta}$  is a summary function with some small  $d_\eta$ . Here we directly compare the empirical distributions of the observations  $y_{1:n}$  and of the synthetic data  $z_{1:n}$ . Other works using measures of similarity between empirical distributions for ABC have been proposed ([Park et al., 2016](#); [Zuluaga et al., 2015](#)). We defer the discussion of the choice of threshold  $\varepsilon$  and algorithmic improvements to Section 5.4. Note that, at each step, we could sample  $z_{1:m}$  with  $m \neq n$ ; the choice  $m = n$  is convenient for drawing connections with existing methods.

The Wasserstein rejection sampler produces draws from the quasi-posterior distribution

$$\pi^\varepsilon(d\theta|y_{1:n}) = \frac{\pi(d\theta) \int_{\mathcal{Y}^n} \mu_\theta^{(n)}(dz_{1:n}) \mathbb{1}(\mathfrak{W}_p(y_{1:n}, z_{1:n}) < \varepsilon)}{\int_{\mathcal{H}} \pi(d\vartheta) \int_{\mathcal{Y}^n} \mu_\vartheta^{(n)}(dz'_{1:n}) \mathbb{1}(\mathfrak{W}_p(y_{1:n}, z'_{1:n}) < \varepsilon)}, \quad (6)$$

where  $\mathbb{1}$  is the indicator function, and where the notation  $\pi^\varepsilon$  hides the choice of the underlying distance  $\rho$  and the order  $p$ . We define the quasi-likelihood as  $q^\varepsilon(\theta) = \int_{\mathcal{Y}^n} \mu_\theta^{(n)}(dz_{1:n}) \mathbb{1}(\mathfrak{W}_p(y_{1:n}, z_{1:n}) < \varepsilon)$ . In certain cases,  $\pi^\varepsilon(d\theta|y_{1:n})$  coincides with more familiar quasi-posterior distributions, as illustrated in the following examples.

**Example 2.3** (Categorical data). *Suppose that the data are categorical:  $\mathcal{Y} = \{x_i\}_{i=1}^k$  and  $\rho(x, y) = \mathbb{1}(x \neq y)$ . The 1-Wasserstein distance between two empirical distributions on  $\mathcal{Y}$  reduces to the total variation distance ([Pflug and Pichler, 2014](#), pp. 55), given by*

$$\mathfrak{W}_1(y_{1:n}, z_{1:n}) = \frac{1}{2} \sum_{i=1}^k |\hat{p}_i - \hat{q}_i|,$$

where  $\hat{p}_i = \#\{j : y_j = x_i\}/n$ ,  $\hat{q}_i = \#\{j : z_j = x_i\}/n$ , and  $\#$  denotes cardinality. The vectors  $\hat{p}$  and  $\hat{q}$  are sufficient statistics, thus the 1-Wasserstein approach coincides with ABC with sufficient statistics, which itself approximates the Bayesian approach when  $\varepsilon \rightarrow 0$ .

**Example 2.4** (Univariate data). *As can be seen from Eq. (5), in the case of univariate data, the proposed sampler reduces to ABC with order statistics. Using order statistics as a choice of summary within ABC has been suggested in various papers, e.g. [Fearnhead and Prangle \(2012\)](#). The Wasserstein distance perspective leads to a justification of that choice and to extensions to multivariate and dependent data.*

For fixed  $n$ , and for models that generate i.i.d. observations, the quasi-posterior  $\pi^\varepsilon(d\theta|y_{1:n})$  can be shown to converge to the standard posterior  $\pi(d\theta|y_{1:n})$  when  $\varepsilon$  goes to zero; see more precise statements in Section 4.2. This provides some justification for the choice of  $m = n$  for the size  $m$  of the synthetic datasets  $z_{1:m}$  in the rejection sampler, which might otherwise seem arbitrary. Following [Frazier et al. \(2016\)](#), we will consider the asymptotic behavior of  $\pi^\varepsilon(d\theta|y_{1:n})$  when both  $n \rightarrow \infty$  and  $\varepsilon \rightarrow \varepsilon_*$ , for some minimal value  $\varepsilon_*$ ; we establish concentration of the quasi-posterior around  $\theta_*$ , the minimizer of  $\theta \mapsto \mathfrak{W}_p(\mu_*, \mu_\theta)$ , in Section 4.2.

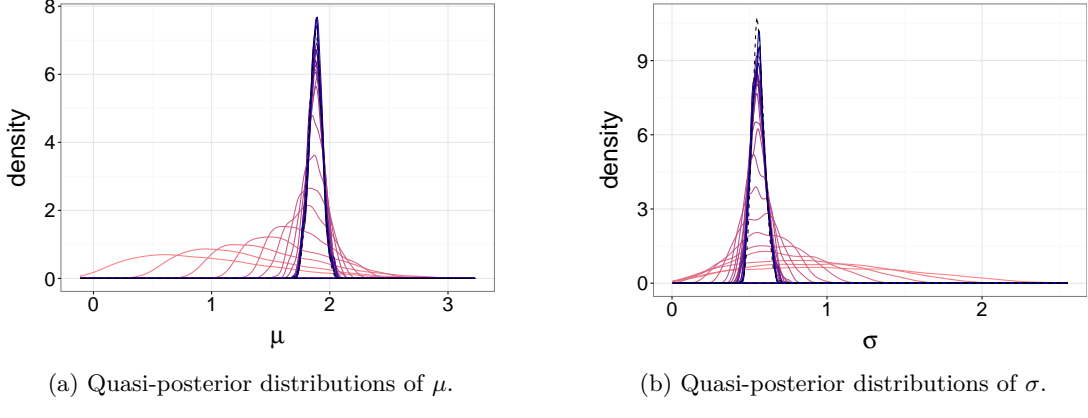


Figure 3: Posterior distribution of  $\mu$  (left) and  $\sigma$  (right) in dashed lines, and quasi-posterior distributions for different  $\varepsilon$  in full lines (colors from light red to dark blue as  $\varepsilon$  decreases). These plots correspond to Example 2.5.

**Example 2.5.** Consider Example 2.1 with  $n = 100$ . The prior is standard Normal on  $\mu$  and Gamma with shape 2 and rate 1 on  $\sigma$ . Figure 3 shows the standard posterior distribution, and the quasi-posterior distributions obtained for different values of  $\varepsilon$ , with the algorithm described in Section 5.4. The quasi-posteriors are seen to converge to the posterior when  $\varepsilon \rightarrow 0$ .

### 3 Dependent data

Since the proposed approach is based on the comparison of empirical distributions, it might seem at first inapplicable to dependent data, for which the order matters. Despite  $\mu_*^{(n)}$  not being a product distribution in such situations,  $\hat{\mu}_n$  might still converge to some distribution  $\mu_*$ . The issue is that the empirical distribution might not contain enough information to identify certain parameters, as illustrated in the following example.

**Example 3.1.** Consider a stationary autoregressive process of order 1, written  $AR(1)$ , where  $y_1 \sim \mathcal{N}(0, \sigma^2/(1-\phi^2))$ , for some  $\sigma > 0$  and  $\phi \in (-1, 1)$ . For each  $t \geq 2$ , let  $y_t = \phi y_{t-1} + \sigma w_t$ , where  $w_t \sim \mathcal{N}(0, 1)$  are independent. The marginal distribution of each  $y_t$  is  $\mathcal{N}(0, \sigma^2/(1-\phi^2))$ . One can show that the empirical distribution of autoregressive time series converges to this marginal distribution, from which the two parameters  $(\phi, \sigma^2)$  are not identifiable. Figure 4a shows quasi-posterior samples, obtained for decreasing values of  $\varepsilon$  with the algorithm described in Section 5.4. The prior is uniform on  $[-1, 1]$  for  $\phi$ , and standard Normal on  $\log(\sigma)$ . The data are generated using  $\phi = 0.7, \log(\sigma) = 0.9$  and  $n = 1,000$ . The quasi-posteriors concentrate on a ridge of values with constant  $\sigma^2/(1-\phi^2)$ .

We propose two approaches to help parameter identifiability in time series data: delay reconstruction and residual reconstruction. Other approaches are possible: for instance, a simple approach would consist in augmenting the times series with the time indices, thus defining  $\bar{y}_t = (t, y_t)$ . The Wasserstein distance between two samples  $\bar{y}_{1:n}$  and  $\bar{z}_{1:n}$  could be used for inference, upon defining a distance on the space  $\{1, \dots, n\} \times \mathcal{Y}$  of  $(t, y_t)$ . We do not explore this approach further.

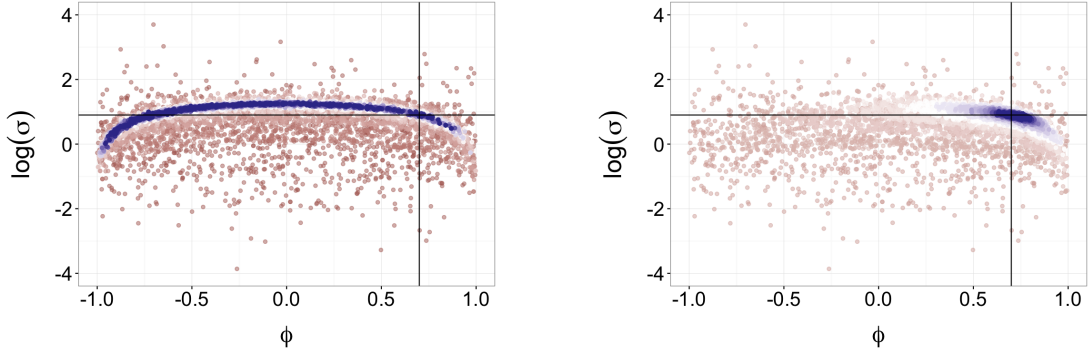


Figure 4: Quasi-posterior samples of  $(\phi, \log(\sigma))$  in the AR(1) example (colors from red to white to blue as  $\varepsilon$  decreases). On the left, using the empirical distribution of the time series, the quasi-posteriors concentrate around a ridge of values such that  $\sigma^2/(1 - \phi^2)$  is constant. On the right, using delay reconstruction with lag  $k = 1$ , the quasi-posteriors concentrate around the data-generating parameters,  $\phi = 0.7, \log(\sigma) = 0.9$ , indicated by full lines. These plots correspond to Examples 3.1 and 3.2.

### 3.1 Delay reconstruction

The idea of delay reconstruction originates in the dynamical systems literature (e.g. [Kantz and Schreiber, 1997](#)), and introduces the lagged values  $\tilde{y}_t = (y_t, y_{t-1}, \dots, y_{t-k})$ , for some lag  $k \in \mathbb{N}$ . The lagged series  $\tilde{y}_{k+1:n}$  inherits many properties, such as stationarity and limiting behavior, from the original series. Therefore the empirical distribution of  $\tilde{y}_{k+1:n}$  might also converge to a limit, which, unlike  $\mu_*$ , captures some aspects of the dependency structure of the observations. This was used in conjunction with Wasserstein distances in [Moeckel and Murray \(1997\)](#); [Musculus and Verduyn-Lunel \(2011\)](#). For our purposes, more parameters might be identifiable from the empirical distribution of  $\tilde{y}_{k+1:n}$  than from the empirical distribution of  $y_{1:n}$ . A Wasserstein rejection sampler targeting the quasi-posterior based on delay reconstruction goes as follows.

1. Draw a parameter  $\theta$  from the prior distribution  $\pi$ . Draw a synthetic dataset  $z_{1:n} \sim \mu_\theta^{(n)}$ . Construct the delay reconstruction  $\tilde{z}_{k+1:n}$  using a lag  $k$ :  $\tilde{z}_t = (z_t, z_{t-1}, \dots, z_{t-k})$  for all  $k+1 \leq t \leq n$ .
2. If  $\mathfrak{W}_p(\tilde{y}_{k+1:n}, \tilde{z}_{k+1:n}) \leq \varepsilon$ , keep the parameter  $\theta$ , otherwise reject it.

**Example 3.2** (Example 3.1 continued). *Using  $k = 1$  in the AR(1) example, consider the delay reconstruction  $\tilde{y}_t = (y_t, y_{t-1})$  for  $t \geq 2$ . The stationary distribution of  $\tilde{y}_t$  is given by*

$$\mathcal{N} \left( \begin{pmatrix} 0 \\ 0 \end{pmatrix}, \frac{\sigma^2}{1 - \phi^2} \begin{pmatrix} 1 & \phi \\ \phi & 1 \end{pmatrix} \right). \quad (7)$$

*The two parameters  $\sigma^2$  and  $\phi$  can be identified from a sample approximating the above distribution. Figure 4b shows quasi-posterior samples obtained with delay reconstruction, for decreasing  $\varepsilon$ . The distributions concentrate around the data-generating values.*

Delay reconstructions (or embeddings) play a central role in dynamical systems, and have desirable theoretical properties as outlined in Takens' theorem ([Takens, 1981](#)) and variants thereof ([Stark et al., 2003](#)). One might also want to consider delay reconstructions of the form  $\check{y}_t = (y_t, y_{t-\tau}, \dots, y_{t-\tau k})$  for some

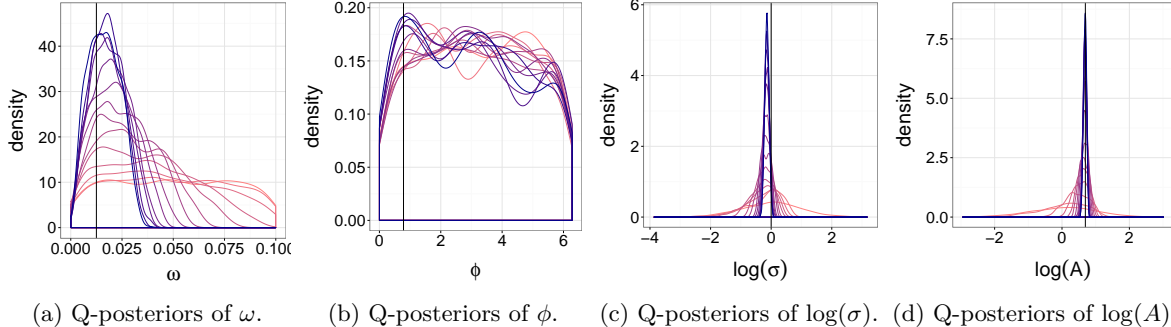


Figure 5: Quasi-posterior distributions of  $(\omega, \phi, \log(\sigma), \log(A))$  (from left to right), using delay reconstruction with lag  $k = 3$ ; each full line corresponds to a value of  $\varepsilon$  (decreasing as the color goes from light red to dark blue). Data-generating parameters are indicated by vertical full lines. These plots correspond to Example 3.3.

$\tau > 1$ . Chapters 3 and 9 in [Kantz and Schreiber \(1997\)](#) provide an overview of methods proposed to choose values of  $k$  and  $\tau$ .

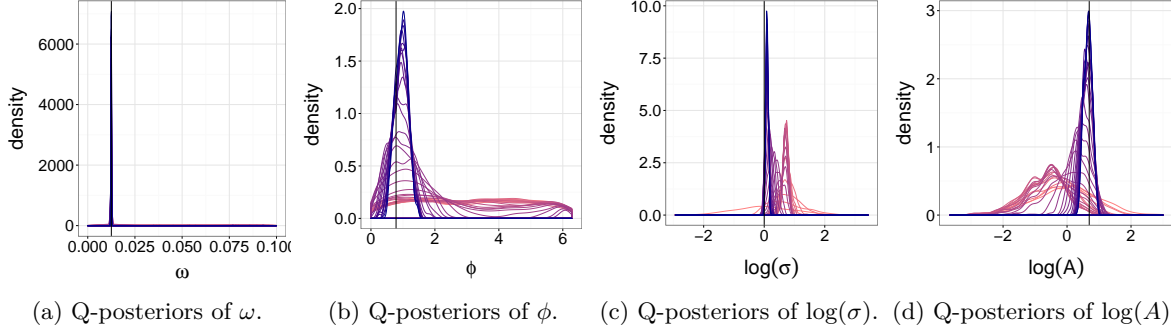
Contrasting the minimum distance approach based on delay reconstructions with likelihood-based estimation, we expect, in general, a loss of information. In any case, it is no longer true that the quasi-posterior  $\pi^\varepsilon(d\theta|y_{1:n})$  converges to the standard posterior  $\pi(d\theta|y_{1:n})$  when  $\varepsilon$  goes to zero. Indeed, the order of the data is only partly reflected in the empirical distribution of  $\tilde{y}_{k+1:n}$ . If some parameters are identified only through that order, then we might not be able to retrieve them with the proposed approach, as in the following example.

**Example 3.3.** Consider the “cosine” model  $y_t = A \cos(2\pi\omega t + \phi) + \sigma w_t$ , where  $w_t \sim \mathcal{N}(0, 1)$  for all  $t \geq 1$  are independent. The parameter  $\phi$  is the phase shift. The information about  $\phi$  is mostly lost when considering arbitrary permutation of the series  $\tilde{y}_{k+1:n}$ , for small values of  $k$ . Therefore, the empirical distribution of  $\tilde{y}_{k+1:n}$  might only contain enough information to identify  $A$ ,  $\omega$  and  $\sigma^2$ . Figure 5 shows the quasi-posteriors of each parameter, for decreasing values of  $\varepsilon$ . The prior distributions are set to uniforms on  $[0, 1/10]$  and  $[0, 2\pi]$  for  $\omega$  and  $\phi$ , and standard Normal on  $\log(\sigma)$  and  $\log(A)$ . The data of size  $n = 500$  are generated using  $\omega = 1/80$ ,  $\phi = \pi/4$ ,  $\log(\sigma) = 0$  and  $\log(A) = \log(2)$ .

We emphasize that, even when time series are univariate, their delay reconstructions are multivariate for any  $k \geq 1$ , so that methods to compute distances between multivariate empirical distributions are required.

### 3.2 Residual reconstruction

Another approach to handle dependent data is advocated in [Mengersen et al. \(2013\)](#), in the context of ABC via empirical likelihood. In many time series models, the observations are seen as transformations of some parameter  $\theta$  and residual variables  $w_1, \dots, w_n$ . Then, given a parameter  $\theta$ , one might be able to reconstruct the residuals corresponding to the observations. In Example 3.3, one can define  $w_t = (y_t - A \cos(2\pi\omega t + \phi))/\sigma$ . Residuals can also be constructed in the AR(1) model of Example 3.1, by defining  $w_t = (y_t - \phi y_{t-1})/\sigma$ , or in ARCH and GARCH models as described in [Mengersen et al. \(2013\)](#). Once residuals have been constructed, their empirical distribution can be compared to the distribution that they would follow under the model, e.g. a standard Normal in Examples 3.1 and 3.3. A Wasserstein rejection sampler using residual reconstruction goes as follows.



(a) Q-posteriors of  $\omega$ . (b) Q-posteriors of  $\phi$ . (c) Q-posteriors of  $\log(\sigma)$ . (d) Q-posteriors of  $\log(A)$ .

Figure 6: Quasi-posterior distributions of  $(\omega, \phi, \log(\sigma), \log(A))$  (from left to right), using residual reconstruction, combined with delay reconstruction with lag  $k = 1$ ; each full line corresponds to a value of  $\varepsilon$  (decreasing as the color goes from light red to dark blue). Data-generating parameters are indicated by vertical full lines. These plots correspond to Example 3.4.

1. Draw a parameter  $\theta$  from the prior distribution  $\pi$ . Construct the residuals  $w_{1:n}$  corresponding to  $y_{1:n}$  and  $\theta$ , and draw  $w'_{1:n}$  from the distribution of the residuals specified by the model.
2. If  $\mathfrak{W}_p(w_{1:n}, w'_{1:n}) \leq \varepsilon$ , keep the parameter  $\theta$ , otherwise reject it.

Even when the model is such that the above residual reconstruction can be implemented, parameter identifiability is not guaranteed. In case of lack of identifiability, one can try to combine both residual and delay reconstructions. Upon constructing the residuals  $w_{1:n}$  and simulating  $w'_{1:n}$ , one can consider the lagged series  $\tilde{w}_{k+1:n}$  and  $\tilde{w}'_{k+1:n}$ , for  $k \geq 1$ , and compute the Wasserstein distance between their empirical distributions. This proves fruitful in the cosine model example.

**Example 3.4** (Example 3.3 continued). *Applying residual reconstruction directly to the cosine model of Example 3.3 results in quasi-posterior distributions that are flat for both  $\omega$  and  $\phi$ . However, by combining residual and delay reconstruction with  $k = 1$ , we obtain better identifiability than using either technique. Figure 6 shows quasi-posteriors for each parameter, for decreasing values of  $\varepsilon$ . Compared to the sole use of delay reconstruction as in Figure 5, the shift parameter  $\phi$  is now identified. The frequency parameter  $\omega$  is also more precisely identified. Remarkably, the distributions of  $\log \sigma$  and  $\log A$  concentrate around slightly off values when  $\varepsilon$  first decreases, before shifting towards the actual data-generating values as  $\varepsilon$  decreases further.*

## 4 Asymptotic properties

We establish conditions for the existence, measurability and consistency of the minimum Wasserstein and minimum expected Wasserstein estimators. Bassetti et al. (2006) study these questions for estimators derived from minimizing a class of optimal transport costs that contains the MWE as the most important special case, but only for well-specified models with i.i.d. data. We draw inspiration from their approach, while extending the results to both the MWE and the MEWE, under misspecified models generating certain types of non-i.i.d. data.

Central to the argument is the assumption that  $\mathfrak{W}_p(\hat{\mu}_n, \mu_*) \rightarrow 0$   $\mathbb{P}$ -almost surely, for some  $\mu_*$ . We also assume that for any  $\theta$ , the synthetic data-generating process  $\mu_\theta^{(n)}$  defines an identifiable distribution  $\mu_\theta$ , informally referred to as the model. In the i.i.d. setting,  $\mu_*$  and  $\mu_\theta$  are simply the marginal distributions

of the observed and synthetic data. In non-i.i.d. settings, they might be the stationary or limiting marginal distributions of delay reconstructed time series, as in Section 3. As such, in this section, we take  $\mathcal{Y}$  to denote a generic space in which our (potentially reconstructed) observations lie.

Beyond consistency, a study of asymptotic distributions is presented in Bassetti and Regazzini (2006) for location-scale models on  $\mathbb{R}$ , in the case where  $p = 1$ , the metric is Euclidean, and the model is well-specified. We extend these results to cover generic models under similar conditions. Finally, we consider the behavior of the quasi-posterior distribution introduced in Section 2.4, when  $\varepsilon \rightarrow 0$  for fixed  $n$ , and when  $\varepsilon$  decreases as  $n$  increases, following existing results on ABC (Frazier et al., 2016).

All proofs can be found in the self-contained supplementary materials.

## 4.1 Minimum Wasserstein estimator

### 4.1.1 Existence, measurability, and consistency

Our first assumption concerns the identifiability of the model.

**Assumption 4.1.** *The map  $\theta \mapsto \mu_\theta$  is injective.*

A sequence of measures  $\mu_n \in \mathcal{P}_p(\mathcal{Y})$  is said to converge weakly in  $\mathcal{P}_p(\mathcal{Y})$  to  $\mu \in \mathcal{P}_p(\mathcal{Y})$  as  $n \rightarrow \infty$  if  $\mu_n \xrightarrow{w} \mu$ , i.e. converges weakly in the usual sense, and there exists  $y_0 \in \mathcal{Y}$  such that  $\int_{\mathcal{Y}} \rho(y, y_0)^p d\mu_n(y) \rightarrow \int_{\mathcal{Y}} \rho(y, y_0)^p d\mu(y)$ . The  $p$ -Wasserstein distance metrizes weak convergence in  $\mathcal{P}_p(\mathcal{Y})$ : a sequence  $\mu_n$  converges weakly to  $\mu$  in  $\mathcal{P}_p(\mathcal{Y})$  if and only if  $\mathfrak{W}_p(\mu_n, \mu) \rightarrow 0$  (Villani (2008), Theorem 6.9). This result is the main tool in establishing the following assumption, which is the only assumption we place on the data-generating process.

**Assumption 4.2.** *The data-generating process is such that  $\mathfrak{W}_p(\hat{\mu}_n, \mu_*) \rightarrow 0$ ,  $\mathbb{P}$ -almost surely, as  $n \rightarrow \infty$ .*

Our results do not assume that the model is well-specified, but assume the existence, uniqueness, and well-separation of  $\theta_* = \operatorname{arginf}_{\theta \in \mathcal{H}} \mathfrak{W}_p(\mu_*, \mu_\theta)$ .

**Assumption 4.3.** *For all  $\varepsilon > 0$ , there exists  $\delta > 0$  such that*

$$\inf_{\theta \in \mathcal{H}: \mathfrak{W}_p(\mu_\theta, \mu_{\theta_*}) \geq \varepsilon} \mathfrak{W}_p(\mu_*, \mu_\theta) > \mathfrak{W}_p(\mu_*, \mu_{\theta_*}) + \delta.$$

The above assumption is akin to those made in the study of the asymptotic properties of the maximum likelihood estimator under misspecification, where  $\theta_*$  is defined in terms of the KL divergence.

**Assumption 4.4.** *For some  $\varepsilon > 0$ , the set  $\tilde{B}_{\theta_*}(\varepsilon) = \{\theta \in \mathcal{H} : \mathfrak{W}_p(\mu_{\theta_*}, \mu_\theta) \leq \varepsilon\}$  is relatively compact, i.e. its closure is compact.*

**Assumption 4.5.**  *$\rho_{\mathcal{H}}(\theta_n, \theta) \rightarrow 0$  implies  $\mu_{\theta_n} \xrightarrow{w} \mu_\theta$ .*

We state results on the existence, measurability, and consistency of the MWE. Similar results for the MEWE are stated in Appendix A, along with an additional assumption. An extra result also states that the MEWE converges to the MWE as  $m \rightarrow \infty$ . The assumptions presented above are formulated on the map  $\theta \mapsto \mu_\theta$  and the parameter space  $\mathcal{H}$ . In the supplementary materials, we present alternative conditions made on the model as a subset of  $\mathcal{P}_p(\mathcal{Y})$  directly. These are slightly more general, but might be harder to work with in practice. Also in the supplementary materials are propositions establishing practical conditions under which Assumptions 4.2 and 4.3 hold.

**Proposition 4.1** (Existence of the MWE). *Under Assumptions 4.2-4.5, there exists a set  $E$  with  $\mathbb{P}(E) = 1$  such that, for all  $\omega \in E$ , there exists  $n(\omega)$  such that, for all  $n \geq n(\omega)$ , there exists  $\hat{\theta}_n(\omega)$  satisfying*

$$\hat{\theta}_n(\omega) \in \operatorname{arginf}_{\theta \in \mathcal{H}} \mathfrak{W}_p(\hat{\mu}_n(\omega), \mu_\theta).$$

**Proposition 4.2** (Measurability of the MWE). *Suppose that  $\mathcal{H}$  is a  $\sigma$ -compact Borel measurable subset of  $\mathbb{R}^{d_\theta}$ . Under Assumptions 4.1-4.5, there exists a Borel measurable version of the MWE.*

**Theorem 4.1** (Consistency of the MWE). *Under Assumptions 4.1-4.5, any  $\hat{\theta}_n$  satisfying Proposition 4.1 converges to  $\theta_\star$   $\mathbb{P}$ -almost surely as  $n \rightarrow \infty$ .*

In the following examples, our assumptions are easily verified. The first one considers a misspecified model, and the second one considers a model with dependent data.

**Example 4.1.** Let  $\mathcal{H} = \mathcal{Y} = \mathbb{R}^m$ ,  $\rho_{\mathcal{H}}(x, y) = \rho(x, y) = \|x - y\|$  be the usual Euclidean distance, and  $p = 2$ . Let  $\mu_\star \in \mathcal{P}_2(\mathbb{R}^m)$ . Consider the location family  $\mathcal{M} = \{\mu_\theta : \theta \in \mathcal{H}\}$ , where  $Y \sim \mu_0$  has mean zero and  $Y + \theta \sim \mu_\theta$ . Suppose  $\mu_\star \notin \mathcal{M}$  and that  $\mu_\star$  has mean equal to  $\theta_\star$ . By Lemma 8.8 in [Bickel and Freedman \(1981\)](#),

$$\mathfrak{W}_2^2(\mu_\star, \mu_\theta) = \|\theta - \theta_\star\|^2 + \mathfrak{W}_2^2(\mu_0, \mu_\star^0),$$

where  $\mu_\star^0$  is the centered version of  $\mu_\star$ . Therefore,  $\theta_\star$  uniquely minimizes  $\theta \mapsto \mathfrak{W}_2(\mu_\star, \mu_\theta)$  and is well-separated. Note also that  $\{\theta \in \mathbb{R}^m : \|\theta - \theta_\star\| \leq \varepsilon\}$  is compact. The preceding results can then be used to establish the existence, measurability, and consistency of the estimators. In this case, the MWE actually corresponds to the sample mean of the observed data, whereas the MEWE does not seem to have an easily accessible closed-form expression.

**Example 4.2.** Consider the data-generating mechanism of the autoregressive process, as in Examples 3.1-3.2. By [Chanda \(1974\)](#) and technical lemmas that can be found in the supplementary materials, the empirical measure of  $\tilde{y}_{2:n}$  converges weakly to its stationary distribution in  $\mathcal{P}_p(\mathcal{Y}^2)$ . The model  $\mathcal{M} = \{\mathcal{N}(0, \Sigma_{\phi, \sigma^2}) : \phi \in (-1, 1), \sigma^2 > 0\}$ , where  $\Sigma_{\phi, \sigma^2}$  is the covariance matrix in Eq. (7), is identifiable and well-specified. The existence, measurability, and consistency of the estimators then follow.

#### 4.1.2 Asymptotic distribution

Under conditions guaranteeing the consistency of the minimum Wasserstein estimator, we study its asymptotic distribution in the case where  $p = 1$ ,  $\mathcal{Y} = \mathbb{R}$ , and  $\rho(x, y) = |x - y|$ . Recall that under this setup, Eq. (4) gives us that  $\mathfrak{W}_1(\mu, \nu) = \int_0^1 |F_\mu^{-1}(s) - F_\nu^{-1}(s)| ds = \int_{\mathbb{R}} |F_\mu(t) - F_\nu(t)| dt$ . We also assume that the model is well-specified, and that  $\mathcal{H}$  is endowed with a norm:  $\rho_{\mathcal{H}}(\theta_1, \theta_2) = \|\theta_1 - \theta_2\|_{\mathcal{H}}$ .

Our approach to derive asymptotic distributions is directly inspired by [Pollard \(1980\)](#). Let  $F_\theta$ ,  $F_\star$  and  $F_n$  denote the cdfs of  $\mu_\theta$ ,  $\mu_\star$  and  $\hat{\mu}_n$  respectively. Informally, we will show that  $\sqrt{n}W_1(\hat{\mu}_n, \mu_\theta)$  can be approximated by  $\int_{\mathbb{R}} |\sqrt{n}(F_n(t) - F_\star(t)) - \langle \sqrt{n}(\theta - \theta_\star), D_\star(t) \rangle| dt$  near  $\theta_\star$ , for some  $D_\star \in (L_1(\mathbb{R}))^{d_\theta}$ , with  $\langle \theta, u \rangle = \sum_{i=1}^{d_\theta} \theta_i u_i$ . Results in [del Barrio et al. \(1999\)](#) and [Dede \(2009\)](#) give conditions under which  $\sqrt{n}(F_n - F_\star)$  converges to a zero mean Gaussian process  $G_\star$  with given covariance structure, under both independent data and certain classes of dependent data. Heuristically, the distribution of  $\sqrt{n}(\hat{\theta}_n - \theta_\star)$  is then close to that of  $\operatorname{arginf}_{u \in \mathcal{H}} \int_{\mathbb{R}} |G_\star(t) - \langle u, D_\star(t) \rangle| dt$ . We state the result for i.i.d. data, but prove it for also certain classes of non-i.i.d. data in the supplementary materials.

**Theorem 4.2.** Suppose  $Y_i \sim \mu_{\theta_\star}$  i.i.d. for  $\theta_\star$  in the interior of  $\mathcal{H}$ , and that  $\int_0^\infty \sqrt{\mathbb{P}(|Y_0| > t)} dt < \infty$ . Suppose that there exists a non-singular  $D_\star \in (L_1(\mathbb{R}))^{d_\theta}$  such that

$$\int_{\mathbb{R}} |F_\theta(t) - F_\star(t) - \langle \theta - \theta_\star, D_\star(t) \rangle| dt = o(\|\theta - \theta_\star\|_{\mathcal{H}}),$$

as  $\|\theta - \theta_\star\|_{\mathcal{H}} \rightarrow 0$ . If  $\operatorname{arginf}_{u \in \mathcal{H}} \int_{\mathbb{R}} |G_\star(t) - \langle u, D_\star(t) \rangle| dt$  is almost surely unique, the minimum Wasserstein estimator of order 1 satisfies

$$\sqrt{n}(\hat{\theta}_n - \theta_\star) \xrightarrow{w} \operatorname{arginf}_{u \in \mathcal{H}} \int_{\mathbb{R}} |G_\star(t) - \langle u, D_\star(t) \rangle| dt,$$

as  $n \rightarrow \infty$ , where  $G_\star$  is a zero mean Gaussian process with  $\mathbb{E}G_\star(s)G_\star(t) = \min\{F_\star(s), F_\star(t)\} - F_\star(s)F_\star(t)$ .

The theorem aligns with the concentration of the estimators observed in Figures 1-2. Computing confidence intervals using the asymptotic distribution is hard, due to its dependence on unknown quantities. The bootstrap appears as a practical alternative, and its validity is left for future research.

The condition  $\int_0^\infty \sqrt{\mathbb{P}(|Y_0| > t)} dt < \infty$  implies the existence of second moments, and is itself implied by the existence of moments of order  $2 + \varepsilon$  for some  $\varepsilon > 0$  (see e.g. Section 2.9 in [Wellner and van der Vaart, 1996](#)). The uniqueness assumption on the  $\operatorname{arginf}$  can be relaxed by considering convergence to the entire set of minimizing values, as in Section 7 of [Pollard \(1980\)](#). Still, uniqueness can sometimes be established (using e.g. [Cheney and Wulbert, 1969](#)). This approach is taken in [Bassetti and Regazzini \(2006\)](#), who directly show that Theorem 4.2 holds when  $\mathcal{M}$  is a location-scale family supported on a bounded open interval. The existence and form of  $D_\star$  can in many cases be derived if the model is differentiable in quadratic mean ([Le Cam, 1970](#)), which is elaborated upon in the supplementary materials.

Theorem 4.2 also holds for approximations of the MWE, say  $\tilde{\theta}_n$ , provided that  $\tilde{\theta}_n = \hat{\theta}_n + o_{\mathbb{P}}(1/\sqrt{n})$ , as can be seen from its proof. In light of Proposition A.3 in the appendix, there exists a sequence  $m(n)$  such that the MEWE  $\hat{\theta}_{n,m(n)}$  satisfies the conclusion of the theorem, provided that  $m(n)$  increases sufficiently fast. The extension of the theorem to multivariate settings is left for future research; the main difficulty stems from the lack of convenient representation of the Wasserstein distance in such settings.

## 4.2 Wasserstein quasi-posterior

In this section, we consider the behavior of the quasi-posterior distribution in Eq. (6), as  $\varepsilon \rightarrow 0$  for fixed  $n$ , and as  $\varepsilon$  decreases and  $n$  increases simultaneously.

### 4.2.1 Behavior as $\varepsilon \rightarrow 0$ for fixed $n$

The first result states that, for a fixed  $n$  and i.i.d. data, the quasi-posterior distributions approximate the standard posterior distribution as  $\varepsilon \rightarrow 0$ .

**Proposition 4.3.** Suppose that the model generates i.i.d. data, and that  $\mu_\theta$  has a continuous density  $f_\theta$ . Suppose also that  $\sup_{y,\theta} f_\theta(y) < \infty$ . For fixed  $n$  and as  $\varepsilon \rightarrow 0$ , the Wasserstein quasi-posterior converges strongly to the standard posterior.

This proposition explains the behavior observed in Figure 3. For any fixed  $n$ ,  $\mathfrak{W}_p(z_{1:n}, y_{1:n}) = 0$  if and only if  $y_{1:n} = z_{\sigma(1:n)}$  for some permutation  $\sigma$  of  $1 : n$ . For dependent data or non-identically distributed data, this property combined with structure of the likelihood imply that the above proposition does not hold.

### 4.2.2 Concentration as $\varepsilon$ decreases and $n$ increases

For a well-specified model, a generic ABC quasi-posterior  $\tilde{\pi}^\varepsilon$  is said to be consistent for  $\theta_*$  if, for any  $\delta > 0$ ,  $\tilde{\pi}(\{\theta \in \mathcal{H} : \rho_{\mathcal{H}}(\theta, \theta_*) > \delta\} | y_{1:n}) \rightarrow 0$  as  $\varepsilon \rightarrow 0$  and  $n \rightarrow \infty$ . In misspecified models or under inappropriate priors, it might be impossible to take  $\varepsilon \rightarrow 0$ . In these cases we could hope for concentration of the quasi-posterior around  $\theta_*$  when  $\varepsilon \rightarrow \varepsilon_*$ , for some minimal  $\varepsilon_*$ . In this section, we define  $\varepsilon_* = \mathfrak{W}_p(\mu_*, \mu_{\theta_*})$ .

We take inspiration from an approach developed in [Frazier et al. \(2016\)](#), that establishes consistency and concentration rates for a summary statistic-based ABC quasi-posterior distribution. We modify their argument to hold for the Wasserstein quasi-posterior and extend it to cover misspecified models. For real-valued sequences  $a_n$  and  $b_n$ ,  $a_n \lesssim b_n$  denotes  $a_n \leq Cb_n$  for some  $C > 0$ .

The moment and concentration inequalities of [Fournier and Guillin \(2015\)](#) can be used verify the following assumption, similar to one made in [Frazier et al. \(2016\)](#), for i.i.d. data and also certain classes of dependent processes.

**Assumption 4.6.** *For any  $\varepsilon > 0$ , suppose  $\mu_\theta^{(n)}(\mathfrak{W}_p(\mu_\theta, \hat{\mu}_{\theta,n}) > \varepsilon) \leq c(\theta)f_n(\varepsilon)$ , where  $f_n(\varepsilon)$  is a sequence of functions that are non-increasing in  $\varepsilon$  for fixed  $n$  and  $f_n(\varepsilon) \rightarrow 0$  for fixed  $\varepsilon$ , and  $c(\theta)$  is  $\pi$ -integrable and satisfies  $c(\theta) \leq c_0$  for all  $\theta$  with  $\mathfrak{W}_p(\mu_{\theta_*}, \mu_\theta) \leq \delta_0$ , for some  $\delta_0$ .*

The following assumption states that the prior distribution has to put enough mass near  $\theta_*$ .

**Assumption 4.7.** *Suppose that there exists  $L > 0$  such that, for all  $\varepsilon$  small enough,*

$$\pi(\{\theta \in \mathcal{H} : \mathfrak{W}_p(\mu_*, \mu_\theta) \leq \varepsilon + \varepsilon_*\}) \gtrsim \varepsilon^L.$$

**Theorem 4.3.** *Suppose Assumptions 4.2-4.3 and 4.6-4.7 hold. The Wasserstein quasi-posterior with threshold  $\varepsilon_n + \varepsilon_*$  satisfies, for any  $R > 0$ ,*

$$\pi^{\varepsilon_n + \varepsilon_*}(\{\theta \in \mathcal{H} : \mathfrak{W}_p(\mu_*, \mu_\theta) > \varepsilon_* + 4\varepsilon_n/3 + f_n^{-1}(\varepsilon_n^L/R)\} | y_{1:n}) \lesssim \frac{1}{R},$$

whenever  $n \rightarrow \infty$ ,  $\varepsilon_n = o(1)$  and  $f_n(\varepsilon_n) = o(1)$ . Additionally, if Assumptions 4.1 and 4.4-4.5 hold, then the quasi-posterior is consistent for  $\theta_*$ .

*Remark 4.1.* This result gives the rate of concentration of the quasi-posterior on sets of the form  $\{\theta \in \mathcal{H} : \mathfrak{W}_p(\mu_*, \mu_\theta) > \delta + \varepsilon_*\}$ , where  $\varepsilon_* = \mathfrak{W}_p(\mu_*, \mu_{\theta_*})$ , in the sense of [Frazier et al. \(2016\)](#). Under further assumptions on their functional relationship with sets of the form  $\{\theta \in \mathcal{H} : \rho_{\mathcal{H}}(\theta, \theta_*) > \delta\}$ , the proposition can also be used to derive rates of concentration on sets of the latter form, as outlined in the supplementary materials.

## 5 Computational methods

We introduce numerical methods to compute approximations of the minimum Wasserstein and minimum expected Wasserstein estimators, and of the Wasserstein quasi-posterior distributions. At the core of these tasks lies the challenging problem of computing Wasserstein distances.

### 5.1 Computing Wasserstein distances

Using Eq. (5), for one-dimensional empirical distributions of size  $n$ , the cost of computing the exact Wasserstein distance between them is of order  $n \log n$ . In higher dimensions, the cost of the exact computation is

of order  $n^3 \log n$  (e.g. [Burkard et al., 2009](#)). Recent advances in numerical transport introduce approximate algorithms with reduced complexity. Notably, [Cuturi \(2013\)](#); [Cuturi and Doucet \(2014\)](#) use an entropically regularized formulation of the optimal transport program, that allow for the application of Sinkhorn’s algorithm, for a cost of order  $n^2$ . [Genevay et al. \(2016\)](#) use entropic regularization in combination with stochastic gradient descent (SGD) to enable the approximate computation of distances between discrete and continuous probability measures, at similar costs.

We rely on Sinkhorn’s algorithm for our numerical experiments, whenever data are multivariate (e.g. due to delay reconstruction as in Section 3). Following the recommendation in [Cuturi \(2013\)](#), we specify the regularization parameter as a constant divided by the median of the pairwise distances between the two samples. We take that constant to be 20, and we use 100 Sinkhorn iterations for any distance calculation, in all experiments. We have found these values to be conservative, but sensitivity analysis is recommended on a case-by-case basis.

The cost in  $n^2$  for multivariate empirical distributions might still appear prohibitive. We emphasize that this cost is model-free. In the setting of ABC, most of the cost typically lies in the simulation of synthetic data. The added cost of computing Wasserstein distances might be negligible, at least if  $n$  is moderate. Secondly, computational methods for complex models are commonly quadratic in the data length: for instance particle MCMC ([Andrieu et al., 2010](#)), SMC<sup>2</sup> ([Chopin et al., 2013](#)) and related methods for parameter inference in state space models have a quadratic cost. Finally, alternative distances can be employed, such as the sliced Wasserstein distance proposed in [Rabin et al. \(2011\)](#). In the next section, we propose another distance, based on the Hilbert space-filling curve, that can be computed for a cost in  $n \log n$ .

## 5.2 An alternative distance using Hilbert space-filling curves

To take advantage of the dramatic reduction in computational cost when comparing univariate empirical distributions, we propose below a method which amounts to 1) transforming multivariate empirical distributions into univariate empirical distributions using the Hilbert space filling curve and 2) computing the MEWE on the latter. As shown in [Gerber and Chopin \(2015b\)](#); [Schretter et al. \(2016\)](#); [Gerber and Chopin \(2015a\)](#), transformations through the Hilbert space filling curve and its inverse preserve a notion of distance between probability measures.

The Hilbert curve  $H : [0, 1] \rightarrow [0, 1]^{d_y}$  is a (Hölder) continuous mapping from  $[0, 1]$  into  $[0, 1]^{d_y}$ . We can define a pseudo-inverse  $h : [0, 1]^{d_y} \rightarrow [0, 1]$  verifying  $h(H(x)) = x$  for all  $x \in [0, 1]$ . We assume in this subsection that  $\mathcal{Y} \subseteq \mathbb{R}^{d_y}$  is such that there exists a mapping  $\psi : \mathcal{Y} \rightarrow (0, 1)^{d_y}$  verifying, for  $y = (y_1, \dots, y_{d_y}) \in \mathcal{Y}$ ,

$$\psi(y) = (\psi_1(y_1), \dots, \psi_{d_y}(y_{d_y}))$$

where the  $\psi_i$ ’s are continuous and strictly monotone. For instance, if  $\mathcal{Y} = \mathbb{R}^{d_y}$ , one can take  $\psi$  to be the component-wise logistic transformation; see [Gerber and Chopin \(2015b\)](#) for more details. By construction, the mapping  $h_{\mathcal{Y}} := h \circ \psi : \mathcal{Y} \rightarrow (0, 1)$  is one-to-one.

We denote by  $\mu^{h_{\mathcal{Y}}}$  the image of a probability measure  $\mu \in \mathcal{P}(\mathcal{Y})$  by  $h_{\mathcal{Y}}$  and we define the Hilbert projection MEWE as

$$\hat{\theta}_{n,m}^h = \underset{\theta \in \mathcal{H}}{\operatorname{arginf}} \mathbb{E}[\mathfrak{W}_p(\hat{\mu}_n^{h_{\mathcal{Y}}}, \hat{\mu}_{\theta,m}^{h_{\mathcal{Y}}})]. \quad (8)$$

Recall that  $\hat{\mu}_{\theta,m}$  denotes the empirical distribution of a sample drawn from  $\mu_{\theta}^{(m)}$ , and the expectation is taken with respect to that randomness. From an algorithmic point of view, the cost is of order  $\ell$  to evaluate

$h_{\mathcal{Y}}(y_i)$  with accuracy  $2^{-\ell}$ , where in practise  $2^{-\ell}$  is set to the machine precision (e.g.  $\ell = 31$ ).

Alternatively, inspired by Eq. (5) which gives an equivalence between the Wasserstein distance and the distance between sorted samples, we can envision a generalization to multivariate settings by means of the Hilbert curve. More precisely, we define the  $\mathfrak{H}_p$ -distance between the empirical distributions defined by  $y_{1:n}$  and  $z_{1:n}$  by

$$\mathfrak{H}_p(y_{1:n}, z_{1:n}) = \left( \frac{1}{n} \sum_{i=1}^n \rho(y_{\sigma_y(i)}, z_{\sigma_z(i)})^p \right)^{1/p}, \quad (9)$$

where  $\sigma_y$  (resp.  $\sigma_z$ ) is the permutation of  $1 : n$  obtained by mapping the sample  $y_{1:n}$  (resp.  $z_{1:n}$ ) into  $(0, 1)$  using the map  $h_{\mathcal{Y}} : \mathcal{Y} \rightarrow (0, 1)$  and sorting it in increasing order. We will also write  $\mathfrak{H}_p(\hat{\mu}_n, \hat{\nu}_n)$  for  $\mathfrak{H}_p(y_{1:n}, z_{1:n})$ , where  $\hat{\mu}_n$  and  $\hat{\nu}_n$  stand for the empirical distributions supported by  $y_{1:n}$  and  $z_{1:n}$ . Indeed, for any integer  $n \geq 1$  and real number  $p \geq 1$ ,  $\mathfrak{H}_p$  defines a distance on the space of empirical distributions of size  $n$ , as proved in the supplementary materials. The distance could be generalized to samples of unequal sizes. The resulting Hilbert ordering MEWE is then defined as

$$\tilde{\theta}_n^h = \operatorname{arginf}_{\theta \in \mathcal{H}} \mathbb{E}[\mathfrak{H}_p(\hat{\mu}_n, \hat{\mu}_{\theta, n})]. \quad (10)$$

Compared to the distance  $\mathfrak{W}_p(\hat{\mu}_n^{h_{\mathcal{Y}}}, \hat{\mu}_{\theta, m}^{h_{\mathcal{Y}}})$ , the calculation of  $\mathfrak{H}_p(\hat{\mu}_n, \hat{\mu}_{\theta, n})$  could be less expensive, since the latter requires ordering the samples  $y_{1:n}$  and  $z_{1:n}$  along the Hilbert curve, and not computing the exact value of their projections on  $(0, 1)$ . More importantly, available computer programs performing Hilbert curve operations turn out to be more adapted for the Hilbert ordering MEWE of Eq. (10). In particular, we use the implementation provided by the function `hilbert_sort` in [The CGAL Project \(2016\)](#) to compute  $\mathfrak{H}_p$  in the numerical experiments. A drawback of  $\tilde{\theta}_n^h$ , compared to  $\hat{\theta}_{n,m}^h$ , is that its asymptotic properties are harder to analyze. The  $\mathfrak{H}_p$ -distance (or  $\mathfrak{W}_p(\hat{\mu}_n^{h_{\mathcal{Y}}}, \hat{\mu}_{\theta, m}^{h_{\mathcal{Y}}})$ ) can be readily used in place of the Wasserstein distance in quasi-posterior distributions; the advantage lies in the computational cost, reduced to  $n \log n$ .

We show in the supplementary materials that, under the assumption that the model is well-specified, the existence, measurability and consistency results obtained for the standard MEWE (Propositions A.1-A.2 and Theorem A.1) also hold for the Hilbert projection MEWE  $\hat{\theta}_{n,m}^h$ . A result in the supplementary materials initiates the study of the Hilbert ordering MEWE, but we leave a more detailed analysis for future research.

**Example 5.1.** We revisit the AR(1) model of Example 3.2. We use delay reconstruction with a lag  $k = 1$ . Using an algorithm described in Section 5.4, we explore the quasi-posteriors associated with decreasing  $\varepsilon$ , using either the regularized Wasserstein distance as in Section 5.1, or the  $\mathfrak{H}_p$ -distance, with  $p = 2$ . Figure 7 shows that both approaches give very similar results.

### 5.3 Optimization

The exact computation of the MWE  $\hat{\theta}_n = \operatorname{arginf}_{\theta \in \mathcal{H}} \mathfrak{W}_p(\hat{\mu}_n, \mu_{\theta})$  is in general intractable, if only because of the intractability of  $\mathfrak{W}_p(\hat{\mu}_n, \mu_{\theta})$ . We can envision the approximation of this distance based on synthetic samples generated given  $\theta$ . For many generative models, sampling  $z_{1:m}$  from  $\mu_{\theta}^{(m)}$  involves sampling random variables  $U$ , referred to as data-generating variables, and computing  $z_{1:m}$  as a deterministic function of  $\theta$  and  $U$ , denoted by  $z_{1:m}(\theta, U)$ . Given  $U$ , the approximate distance  $\mathfrak{W}_p(y_{1:n}, z_{1:m}(\theta, U))$  is a deterministic function of  $\theta$  which can be numerically optimized. If  $m$  is large, the empirical distribution of  $z_{1:m}$  is expected to be close to  $\mu_{\theta}$ , so that we expect the resulting estimator to be close to the MWE with large probability.

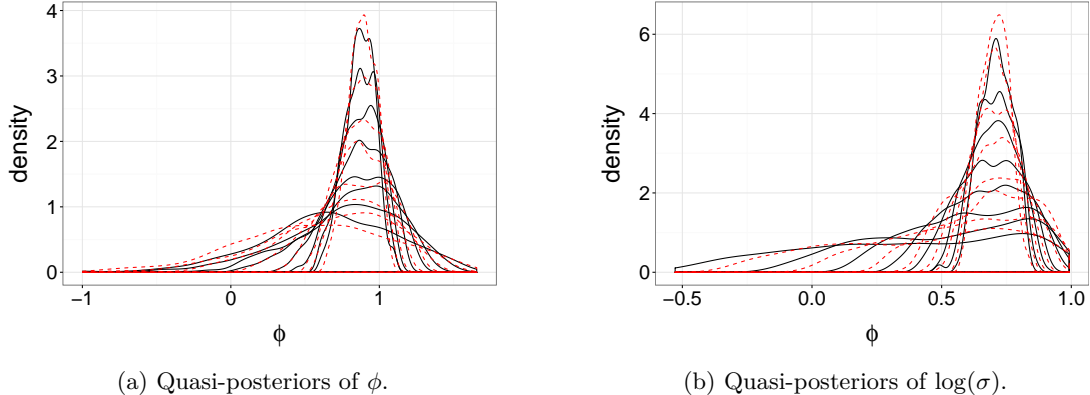


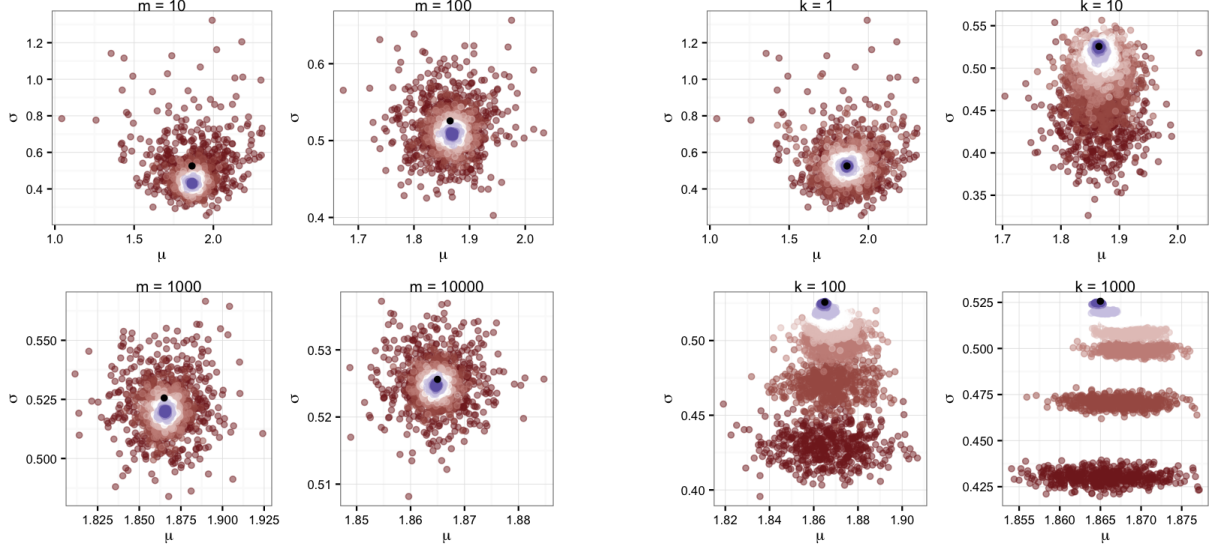
Figure 7: Quasi-posterior distributions of  $\phi$  (left) and of  $\log(\sigma)$  (right) in the AR(1) example, using delay reconstruction with lag  $k = 1$ ; each full black line corresponds to a value of  $\varepsilon$ , obtained using approximated Wasserstein distances. The sampling algorithm is run a second time, using the  $\mathfrak{H}_p$ -distance of Eq. (9), leading to quasi-posteriors represented by red dashed lines.

*Remark 5.1.* The article [Montavon et al. \(2016\)](#) proposes an approximation of the gradient of the function that maps  $\theta$  to an entropy-regularized Wasserstein distance between  $\hat{\mu}_n$  and  $\mu_\theta$ , leveraging the recent advances described in Section 5.1. Unfortunately, it is not applicable in the setting of purely generative models, as it involves point-wise evaluations of the derivative of the log-likelihood.

In order to reduce the variability of the distance approximation, one could average over  $k \geq 1$  replicate datasets, effectively optimizing the approximate distance  $k^{-1} \sum_{i=1}^k \mathfrak{W}_p(y_{1:n}, z_{1:m}(\theta, U^{(i)}))$ , where  $U^{(i)}$  are i.i.d. In the limit  $k \rightarrow \infty$ ,  $k^{-1} \sum_{i=1}^k \mathfrak{W}_p(y_{1:n}, z_{1:m}(\theta, U^{(i)})) \rightarrow \mathbb{E}[\mathfrak{W}_p(\hat{\mu}_n, \hat{\mu}_{\theta, m})]$  almost surely, thus the estimator mimics the MEWE. Experiments for different values of  $k$  and  $m$  are provided in Example 5.2. The optimization of functions defined as expectations is reminiscent of Monte Carlo Expectation-Maximization algorithms ([Wei and Tanner, 1990](#)). Convergence results for these algorithms, as both the number of iterations and the value of  $k$  go to infinity, are reviewed in [Neath et al. \(2013\)](#). The incremental cost of increasing  $k$  is typically lower than that of increasing  $m$ , due in part to the potential for parallelization when calculating the distances  $\mathfrak{W}_p(y_{1:n}, z_{1:m}(\theta, U^{(i)}))$  for a given  $\theta$ , and in part to the algorithmic complexity in  $m$ , which might be super-linear. We can plug in the  $\mathfrak{H}_p$ -distance of Section 5.2 instead of the Wasserstein distance to reduce the cost in multivariate settings.

**Example 5.2.** We revisit Example 2.1, where  $\mu_* = \text{Gamma}(10, 5)$  and  $\mathcal{M} = \{N(\mu, \sigma^2) : \mu \in \mathbb{R}, \sigma > 0\}$ . We fix an observed data set of size  $n = 100$ , and compute  $M = 500$  instances of the approximate MEWE for 8 different values of  $k$  and  $m$ , ranging from 1 to 1,000 and 10 to 10,000 respectively. In Figure 8a, we plot the estimators obtained for all the levels of  $k$ , given 4 different values of  $m$ . In Figure 8b, we plot the estimators obtained for all the levels of  $m$ , given 4 different values of  $k$ . The axis scales are different for each subplot. In both figures, black points correspond to the "true" MWE, calculated using a very large value of  $m$  ( $m = 10^8$ ). For low values of  $m$ , the estimators might be significantly different from the MWE, as can be seen from the lower-right sub-plots of Figure 8b. When  $m$  increases, the estimators converge to the MWE. Increasing  $k$  reduces variation in the estimator, but does not change the objective in such a way that the location of the optimizing parameter approaches the MWE. The changes in  $k$  and  $m$  had no significant impact on the number of evaluations of the objective required to locate the maximum using the `optim` function in R.

In the spirit of Monte Carlo optimization, we can use sampling algorithms, as described in Section 5.4, to



(a) Approximate MEWE across all levels of  $k$  for different values of  $m$ .

(b) Approximate MEWE across all levels of  $m$  for different values of  $k$ .

Figure 8: Samples obtained for different values of  $m$  and  $k$  in the Normal location model of Example 5.2 with Gamma distributed data.

approximate the point estimators  $\hat{\theta}_{n,m}$ . This assumes that the quasi-posterior distribution puts mass around the MEWE, presumably because the effect of the prior is small. Related discussions can be found in [Wood \(2010\)](#); [Rubio et al. \(2013\)](#).

## 5.4 Sampling

We can employ Monte Carlo methods to approximate the quasi-posterior  $\pi^\varepsilon$  defined in Eq. (6). Since point-wise density evaluations of  $\pi^\varepsilon$  can be unbiasedly estimated, the sampling task is an instance of pseudo-marginal problems ([Andrieu and Roberts, 2009](#)). Methods developed in the ABC literature can be translated to the current context. They are typically based on rejection sampling, Markov chain Monte Carlo (MCMC), population or sequential Monte Carlo (SMC) ([Marjoram et al., 2003](#); [Toni et al., 2009](#); [Del Moral et al., 2012](#); [Lee, 2012](#); [Filippi et al., 2013](#)).

### 5.4.1 An adaptive SMC algorithm

We consider an SMC algorithm, which leads to an automatic choice of decreasing thresholds  $(\varepsilon_t)$ , is parallelizable over the particles, and can leverage any MCMC kernel within the rejuvenation step. Choices of Markov kernel and adaptation rule for the thresholds are discussed in Sections 5.4.2 and 5.4.3. For dependent data, the algorithm can be readily modified to include delay and residual reconstructions. We can also use the  $\mathfrak{H}_p$ -distance of Section 5.2 instead of the Wasserstein distance.

Let  $N$  be the number of particles, and  $\varepsilon_0 = \infty$ . The first step goes as follows.

1. Sample  $\theta_0^1, \dots, \theta_0^N$  from the prior  $\pi$ , set  $w_0^k = N^{-1}$  for all  $k \in 1 : N$ .
2. For each  $k \in 1 : N$ , sample  $z_{1:n}^k$  from  $\mu_{\theta^k}^{(n)}$ , and compute the distance  $d_0^k = \mathfrak{W}_p(y_{1:n}, z_{1:n}^k)$ .

3. Based on  $(\theta_0^k)_{k=1}^N$  and  $(d_0^k)_{k=1}^N$ , compute the next threshold  $\varepsilon_1$ .

To approximate  $\pi^{\varepsilon_t}$  based on the samples approximating  $\pi^{\varepsilon_{t-1}}$ , perform the following for  $t \geq 1$ .

1. Define the weight  $w_t^k \propto \mathbb{1}(d_{t-1}^k \leq \varepsilon_t)$  for all  $k \in 1 : N$ , and normalize the weights.
2. Sample ancestor indices  $a_{t-1}^1, \dots, a_{t-1}^N$  such that  $\mathbb{P}(a_{t-1}^k = j) = w_t^j$  for all  $j, k \in 1 : N$ .
3. Sample  $\theta_t^k$  from  $K^{\varepsilon_t}(\theta_{t-1}^{a_{t-1}^k}, \cdot)$ , a Markov kernel leaving  $\pi^{\varepsilon_t}$  invariant, and store the associated distance  $d_t^k$ , for all  $k \in 1 : N$ ; this is the rejuvenation step.
4. Based on  $(\theta_t^k)_{k=1}^N$  and  $(d_t^k)_{k=1}^N$ , compute the next threshold  $\varepsilon_{t+1}$ .

We use systematic resampling to obtain  $a_{t-1}^{1:N}$  at step  $t$ , noting that other resampling schemes exist with varying degrees of parallelism (Murray et al., 2016).

#### 5.4.2 Choice of Markov kernels

Any choice of kernel  $K^\varepsilon$  leaving  $\pi^\varepsilon$  invariant would be valid, the simplest arguably being the kernel of Marjoram et al. (2003), i.e. a standard pseudo-marginal Metropolis–Hastings kernel. This kernel tends to be less and less effective at diversifying the particles as  $\varepsilon$  goes to zero, which can be compensated for by iterating the kernel more and more times. Instead, we use the r-hit kernel of Lee (2012), and Algorithm 6 of that paper in particular, which automatically adapts the computational budget of the kernel to the value of  $\varepsilon$ ; see Lee and Łatuszyński (2014) for a theoretical comparison of MCMC kernels for ABC-type targets. Starting from a value  $\theta$  and an associated distance  $d$ , the kernel works as follows, based on a desired number of hits  $r \geq 2$  and a proposal distribution  $g(\cdot|\theta)$  on the parameter space.

1. For  $i \geq 1$ , sample  $\theta'^i \sim g(\cdot|\theta)$  and  $z_{1:n}^i \sim \mu_{\theta'^i}^{(n)}$ , until  $\sum_{j=1}^i \mathbb{1}(\mathfrak{W}_p(y_{1:n}, z_{1:n}^j) \leq \varepsilon) = r$ . Let  $K' = i$ .
2. Sample uniformly  $L$  among  $\{j \in \{1, \dots, K' - 1\} : \mathbb{1}(\mathfrak{W}_p(y_{1:n}, z_{1:n}^j) \leq \varepsilon)\}$ .
3. For  $i \geq 1$ , sample  $\theta^i \sim g(\cdot|\theta'^L)$  and  $x_{1:n}^i \sim \mu_{\theta^i}^{(n)}$ , until  $\sum_{j=1}^i \mathbb{1}(\mathfrak{W}_p(y_{1:n}, x_{1:n}^j) \leq \varepsilon) = r - 1$ . Let  $K = i$ .
4. With probability

$$\min \left( 1, \frac{\pi(\theta'^L)}{\pi(\theta)} \frac{g(\theta|\theta'^L)}{g(\theta'^L|\theta)} \frac{K}{K' - 1} \right),$$

output  $\theta'^L$  and the distance  $\mathfrak{W}_p(y_{1:n}, z_{1:n}^L)$ ; otherwise output  $\theta$  and  $d$ .

We use  $r = 2$  as a default choice. The proposal distribution  $g(\cdot|\theta)$  can be adapted based on the particles  $(w_t^k, \theta_{t-1}^k)_{k=1}^N$  at step  $t$ , which approximate  $\pi^{\varepsilon_t}$ . By default, we can fit a parametric distribution on the particles, such as a Normal distribution using the empirical mean and covariance matrix of the particles. In the numerical experiments, we define  $g(\cdot|\theta)$  as a mixture of 5 multivariate Normal distributions, fitted on the particles available at step  $t$ , to partially accommodate non-Gaussian features of the target.

#### 5.4.3 Adaptation of thresholds

The SMC framework allows the automatic adaptation of thresholds (see e.g. Del Moral et al. (2012); Silk et al. (2013)). A simple approach consists in choosing  $\varepsilon_{t+1}$  such that the effective sample size computed on the resulting weights  $(w_{t+1}^k)_{k=1}^N$ , defined as  $\text{ESS}_{t+1} = (\sum_{k=1}^N (w_{t+1}^k)^2)^{-1}$ , is above a certain threshold, e.g.  $N/2$ . We use a slightly different approach, motivated by the fact that multiple particles might be identical

at any step  $t \geq 1$  of the SMC sampler. Indeed, the resampling step leads to duplicate values, which the MCMC steps only partially diversify. Criteria that are based solely on the weights fail to account for this potential lack of diversity.

We define a diversity parameter  $\alpha$ , set to 0.5 by default, which indicates the desired minimum proportion of unique particles within our sample, at all steps. The idea is to find  $\varepsilon_{t+1}$  such that, upon resampling the particles using weights  $w_{t+1}^k \propto \mathbb{1}(d_t^k \leq \varepsilon_{t+1})$ , we obtain at least a proportion  $\alpha$  of unique particles. This is complicated by the randomness of the resampling step. Therefore, we clamp that randomness by drawing the uniform variables of the resampling step and keeping them fixed during the calculation of  $\varepsilon_{t+1}$ . The proportion of unique particles after resampling is then a deterministic function of  $\varepsilon$ , denoted by  $f(\varepsilon)$ . We could define  $\varepsilon_{t+1}$  as the value  $\varepsilon$  in the interval  $[0, \varepsilon_t]$  such that  $f(\varepsilon) = \alpha$ . Since that equality might not be achievable, we use a numerical optimizer to minimize  $|f(\varepsilon) - \alpha|$  over  $\varepsilon \in [0, \varepsilon_t]$ .

As a result, the sequence of thresholds  $(\varepsilon_t)$  decreases, but only if the MCMC steps have managed to diversify the particles. We can let the SMC sampler run indefinitely, saving the particles and distances obtained at every step  $t$ , and decide to stop the algorithm if the sequence of thresholds  $(\varepsilon_t)$  does not decrease anymore.

Other Monte Carlo methods could be envisioned to facilitate the exploration of  $\pi^\varepsilon$ , especially for small values of  $\varepsilon$ . One approach is to include the data-generating variables  $U$  (as introduced in Section 5.3) as part of the state space, and to perform alternating updates of the parameters and these variables. This has been explored for pseudo-marginal algorithms (Deligiannidis et al., 2015; Murray and Graham, 2016; Jacob et al., 2016), and specifically for ABC in Prangle et al. (2016). The latter provides an elegant ABC approach without summary statistics, directly using the distance on the observation space to compare observed and synthetic data. We note that including the variables  $U$  can be challenging. For instance, Sections 6.2 and 6.4 contain models for which the data-generating variables  $U$  are not of fixed dimension, as the data mechanisms involve a random number of random variables.

## 6 Numerical experiments

We illustrate the proposed adaptive SMC approach on four examples. The first two involve independent univariate data, for which the Wasserstein distance is computed using Eq. (5) for a cost of  $n \log n$ ; we set the order to  $p = 2$ . The third and fourth examples are state space models, for which we used delay reconstructions, leading to multivariate empirical distributions. We then use the approximation of Wasserstein described in Section 5.1, and the  $\mathfrak{H}_p$ -distance of Section 5.2, for costs in  $n^2$  and  $n \log n$  respectively.

### 6.1 Quantile “g-and-k” distribution

A classical example used in the ABC literature is the g-and-k distribution (see e.g. Fearnhead and Prangle, 2012; Mengersen et al., 2013), where the quantile function is given by

$$r \in (0, 1) \mapsto A + B \left( 1 + c \frac{1 - \exp(-gz(r))}{1 + \exp(-gz(r))} \right) (1 + z(r)^2)^k z(r),$$

where  $z(r)$  refers to the  $r$ -th quantile of the standard Normal distribution, and  $c$  is set to 0.8. The parameters are  $A$ ,  $B$ ,  $g$  and  $k$ , representing location, scale, skewness and kurtosis. Since the distribution is defined through its quantile function, sampling from it is simple but computing its probability density function is difficult.

We generate  $n = 250$  observations from the model using  $A = 3, B = 1, g = 2, k = 0.5$ . We attempt to retrieve these values, using a uniform prior distribution on  $[0, 10]$  for each parameter. Figure 9 shows the output of the SMC sampler with  $N = 2,048$  particles, after 33 steps. From the bivariate marginal plots in Figures 9a and 9b, the quasi-posteriors of  $A, B$  and  $k$  concentrate around the data-generating values, indicated by full lines. For  $g$ , the concentration is not apparent from Figure 9b; thus we plot its marginal quasi-posterior in Figure 9c. We see that the quasi-posterior has a global mode around the data-generating value, for  $\varepsilon$  small enough. The thresholds ( $\varepsilon_t$ ) obtained during the SMC run are shown in Figure 9d. We see that they decrease less and less during the run.

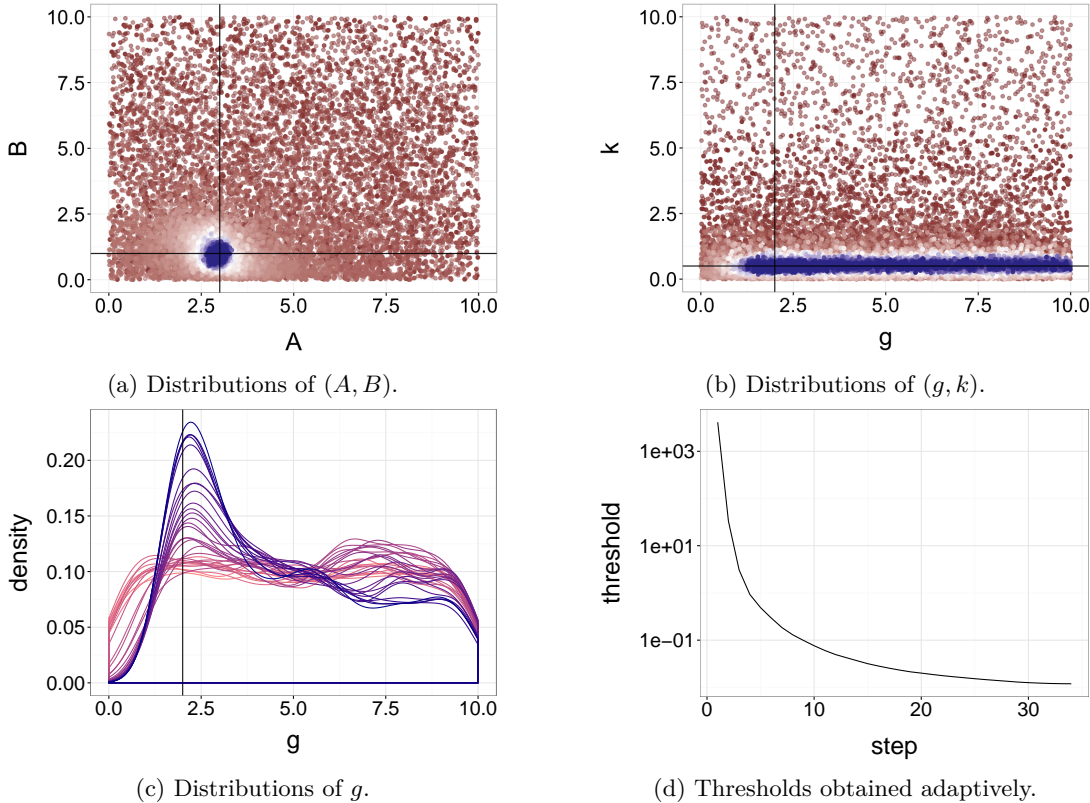


Figure 9: SMC sampler output for the g-and-k quasi-posterior distributions. The top plots show the bivariate marginals of  $(A, B)$  (top left) and  $(g, k)$  (top right). Data-generating values are indicated by full lines. The marginal quasi-posteriors of  $g$  are shown on the bottom left plot, and the sequence of thresholds  $(\varepsilon_t)$  on the bottom right.

## 6.2 Toggle switch model

We borrow the system biology “toggle switch” model used in Bonassi et al. (2011); Bonassi and West (2015), inspired by studies of dynamic cellular networks. The measurements of each cell  $y_i$ , for  $i \in 1 : n$ , are assumed to be independently distributed as Normal variables with mean  $\mu + u_{i,T}$  and standard deviation  $\mu\sigma/u_{i,T}^\gamma$ , where  $\mu, \sigma, \gamma$  are parameters. The value  $u_{i,T}$  is the terminal point of the first component of a bivariate process, denoted by  $(u_{i,t}, v_{i,t})_{t=0}^T$  and defined as follows. Starting from  $(u_{i,0}, v_{i,0}) = (10, 10)$ , the evolution of  $(u_{i,t}, v_{i,t})$  is given by

$$u_{i,t+1} = u_{i,t} + \alpha_1/(1 + v_{i,t}^{\beta_1}) - (1 + 0.03u_{i,t}) + 0.5\xi_{i,1,t},$$

$$v_{i,t+1} = v_{i,t} + \alpha_2/(1 + u_{i,t}^{\beta_2}) - (1 + 0.03v_{i,t}) + 0.5\xi_{i,2,t},$$

where  $\alpha_1, \alpha_2, \beta_1, \beta_2$  are parameters, and  $\xi$ 's are standard Normal variables, truncated so that  $(u_{i,t}, v_{i,t})$  only takes non-negative values. There are seven parameters to estimate in total:  $\alpha_1, \alpha_2, \beta_1, \beta_2, \mu, \sigma, \gamma$ . We do not have access to the data set used in [Bonassi and West \(2015\)](#), so we generate one, with  $n = 2,000$  and using  $T = 300$ . By visual inspection of the figures in [Bonassi and West \(2015\)](#), we use the following parameters to generate plausible data:  $\alpha_1 = 22, \alpha_2 = 12, \beta_1 = 4, \beta_2 = 4.5, \mu = 325, \sigma = 0.25, \gamma = 0.15$ . A histogram of the generated data is given in Figure 10a. Comparing to the real data shown in [Bonassi and West \(2015\)](#), the general bimodal shape is similar, but the two modes seem more separated in our dataset than in the real data.

We consider the task of estimating the data-generating values, using uniform prior distributions on  $[0, 50]$  for  $\alpha_1, \alpha_2$ , on  $[0, 5]$  for  $\beta_1, \beta_2$ , on  $[250, 450]$  for  $\mu$ ,  $[0, 0.5]$  for  $\sigma$  and on  $[0, 0.4]$  for  $\gamma$ . These ranges are derived from Figure 5 in [Bonassi and West \(2015\)](#). Instead of using 11-dimensional tailor-made summary statistics as in [Bonassi et al. \(2011\)](#); [Bonassi and West \(2015\)](#), we use the Wasserstein distance of order 2. The SMC sampler with r-hit moves was run with  $N = 2,048$  for 40 steps.

The seven marginal distributions obtained for various  $\varepsilon$  are shown in Figure 10. We find that the quasi-posterior distributions concentrate at different rates depending on the parameters, similarly to the results of [Bonassi and West \(2015\)](#). These experiments indicate that the design of custom summary statistics can be potentially bypassed.

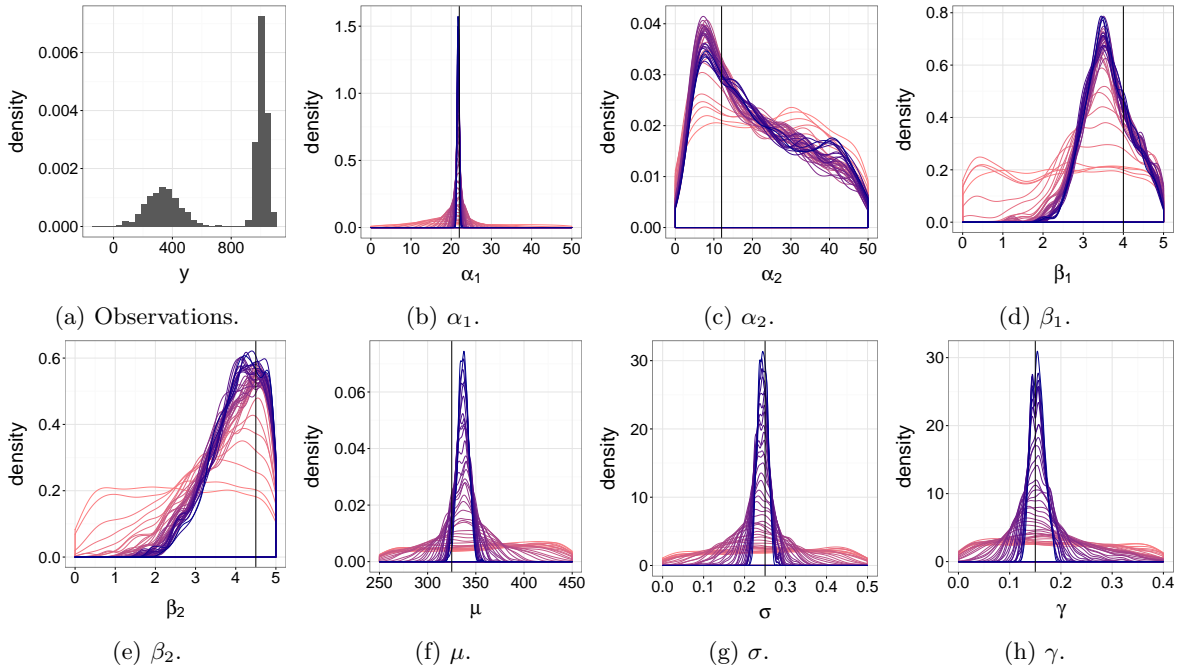


Figure 10: Histogram of observations (top left), and quasi-posterior distributions of parameters in the toggle switch model (all others). Data-generating values are indicated by vertical lines. Different values of  $\varepsilon$ , automatically obtained with the SMC sampler, are indicated by different full lines.

### 6.3 Phytoplankton–zooplankton model

We experiment with the plankton state space model of [Jones et al. \(2010\)](#). A latent process,  $x_t = (p_t, z_t)$  at time  $t$ , represents the population size of phytoplankton and zooplankton. The initial states are given by  $\log p_0 \sim \mathcal{N}(\log 2, 1)$  and  $\log z_0 \sim \mathcal{N}(\log 2, 1)$ . The transition kernel of that process is given by a Lotka–Volterra equation,

$$\frac{dp_t}{dt} = \alpha p_t - cp_t z_t, \quad \text{and} \quad \frac{dz_t}{dt} = ec p_t z_t - m_l z_t - m_q z_t^2,$$

where the growth rate  $\alpha$  follows  $\mathcal{N}(\mu_\alpha, \sigma_\alpha^2)$  at every integer time  $t$ . The equation is solved numerically using a Runge–Kutta method. The data ( $y_t$ ) are noisy measurements of  $p_t$ :  $\log y_t \sim \mathcal{N}(\log p_t, 0.2^2)$ . The parameters are  $(\mu_\alpha, \sigma_\alpha, c, e)$ , and we keep  $m_l$  and  $m_q$  fixed to the value 0.1. Parameter inference for this type of state space models would typically be done with particle MCMC methods ([Andrieu et al., 2010](#); [Jones et al., 2010](#)), or iterated filtering ([Ionides et al., 2015](#)).

We generate  $T = 250$  observations using  $\mu_\alpha = 0.7$ ,  $\sigma_\alpha = 0.4$ ,  $c = 0.25$ ,  $e = 0.3$ . We specify a uniform prior on  $[0, 1]$  for all four parameters. We use a lag of  $k = 3$  for delay reconstructions, the Wasserstein distance of order 2, and  $N = 1,024$  particles in the SMC sampler. The bivariate marginal quasi-posteriors are given in Figure 11. Some parameters are more accurately retrieved than others:  $\sigma_\alpha$  is somewhat recovered,  $\mu_\alpha$  less so, and the distributions of  $(c, e)$  concentrate around a ridge. We have experimented with different values of the lag  $k$ , and with the  $\mathfrak{H}_p$ -distance of Section 5.2 with longer data sets, and have obtained qualitatively similar results. Therefore, the method of delay reconstruction does not lead to accurately identified parameters in this example. The resulting samples could still be used to start Markov chains or numerical optimizers, as they are closer to the data-generating values than random draws from the prior.

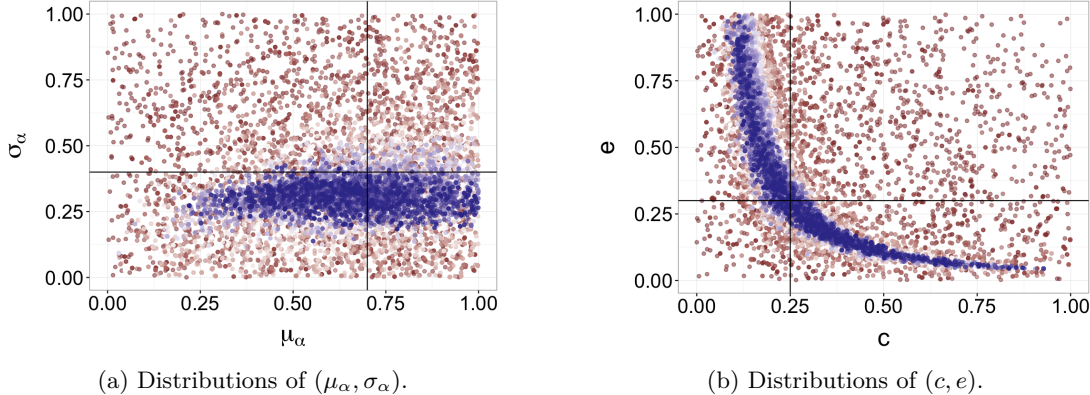


Figure 11: SMC sampler output for the plankton model. The plots show the bivariate marginals of  $(\mu_\alpha, \sigma_\alpha)$  (left) and  $(c, e)$  (right). Data-generating parameter values are indicated by full lines.

### 6.4 Lévy-driven stochastic volatility model

We consider a Lévy-driven stochastic volatility model as introduced by [Barndorff-Nielsen and Shephard \(2001\)](#), and used in [Chopin et al. \(2013\)](#) as an example of state space model that is challenging to calibrate. The observations  $y_{1:n}$  are the log-returns of some financial asset, assumed to be Normal with mean  $\mu + \beta v_t$  and variance  $v_t$  at time  $t$ , where  $v_t$  is the actual volatility process. Together with the spot volatility denoted by  $z_t$ ,  $(v_t, z_t)$  constitutes the latent process, assumed to follow a Lévy process. Starting with  $z_0 \sim \Gamma(\xi^2/\omega^2, \xi/\omega^2)$

(where the second parameter is the rate), and an arbitrary  $v_0$ , the evolution of the process goes as follows:

$$\begin{aligned} k &\sim \text{Poisson} \left( \lambda \xi^2 / \omega^2 \right), \quad c_{1:k} \stackrel{\text{i.i.d.}}{\sim} \mathcal{U}(t, t+1), \quad e_{1:k} \stackrel{\text{i.i.d.}}{\sim} \text{Exp} \left( \xi / \omega^2 \right), \\ z_{t+1} &= e^{-\lambda} z_t + \sum_{j=1}^k e^{-\lambda(t+1-c_j)} e_j, \quad v_{t+1} = \frac{1}{\lambda} \left[ z_t - z_{t+1} + \sum_{j=1}^k e_j \right] \end{aligned} \quad (11)$$

The random variables  $(k, c_{1:k}, e_{1:k})$  are generated independently for each time period, and  $1 : k$  is the empty set when  $k = 0$ . The parameters are  $(\mu, \beta, \xi, \omega^2, \lambda)$ . We specify the prior as Normal with mean zero and variance 2 for  $\mu$  and  $\beta$ , Exponential with rate 0.2 for  $\xi$  and  $\omega^2$ , and Exponential with rate 1 for  $\lambda$ .

We generate synthetic data with  $n = 10,000$ ,  $\mu = 0$ ,  $\beta = 0$ ,  $\xi = 0.5$ ,  $\omega^2 = 0.0625$ ,  $\lambda = 0.01$ , which were used also in the simulation study of [Barndorff-Nielsen and Shephard \(2002\)](#); [Chopin et al. \(2013\)](#). We use delay reconstruction with a lag  $k = 1$ , which makes the reconstructed data bivariate. Given the length  $n$ , we use the  $\mathfrak{H}_p$ -distance of Section 5.2 (with  $p = 1$ ), with a cost in  $n \log n$ . The SMC sampler was run for 40 steps with  $N = 1,024$  particles. Figure 12 shows the resulting quasi-posterior marginals for  $(\mu, \beta)$ ,  $(\xi, \omega^2)$ , and  $\lambda$ . One can see that the parameters  $(\mu, \beta, \xi, \omega^2)$  are accurately recovered. On the other hand, the marginal distribution of  $\lambda$  has shifted towards the data-generating value, but is still far from being concentrated around it. Overall, the method manages to find regions close to the data-generating values in this example, for a cost in  $n \log n$  thanks to the  $\mathfrak{H}_p$ -distance. This is less expensive than currently available methods for state space models. Again, the resulting samples could be used, at least, for initializing a subsequent Markov chain or numerical optimizer.

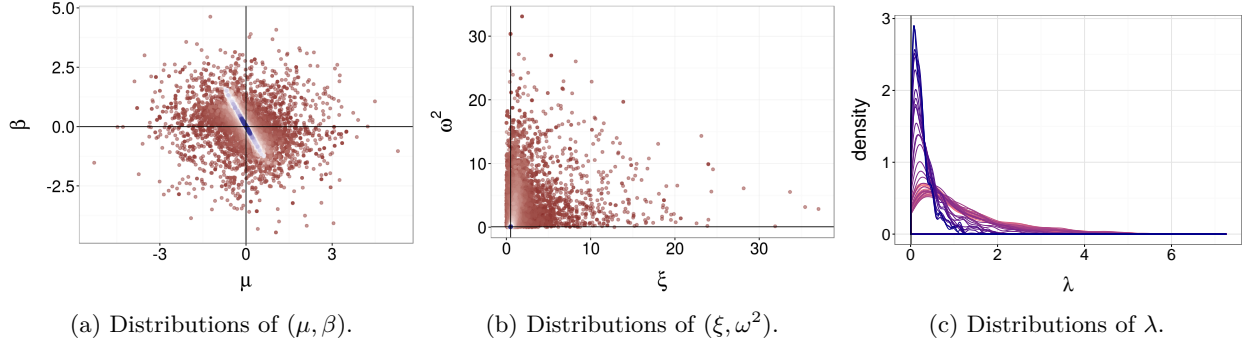


Figure 12: SMC sampler output for the Lévy-driven stochastic volatility model. The plots show the bivariate marginals of  $(\mu, \beta)$  (left),  $(\xi, \omega^2)$  (middle), and the marginal distributions of  $\lambda$  (right). Data-generating parameter values are indicated by full lines.

## 7 Discussion

The Wasserstein distance can be useful to perform statistical inference in purely generative models. The Wasserstein distance is based on a distance on the data space, which needs to be chosen by the user. This might be considered either an advantage or a hindrance. The choice of distance on the observation space and of order  $p$  has an impact, as seen in Example 2.2 with a Normal model on Cauchy data.

The minimum Wasserstein estimator has been theoretically studied in [Bassetti et al. \(2006\)](#). We have extended these results by considering minimum expected Wasserstein estimators, misspecified settings and certain classes of dependent data. Furthermore, we have studied asymptotic properties of the associated

quasi-posterior distributions, following the work of Frazier et al. (2016). One way of constructing confidence intervals for MWE and MEWE is via the bootstrap; this would be an interesting avenue of research.

The  $\mathfrak{H}_p$ -distance of Section 5.2 provides a convenient alternative to the Wasserstein distance when the computation of the latter is prohibitively costly, particularly for large data sets. The good numerical performance of the  $\mathfrak{H}_p$ -distance motivates further theoretical study of its properties, as initiated in the supplementary materials.

Using an SMC algorithm, with r-hit MCMC kernels, threshold adaptation and independent proposals fitted on the particles, the algorithmic tuning is minimal. Some tuning values, such as the minimum desired diversity  $\alpha$  of Section 5.4.3 and the number of hits  $r$  of Section 5.4.2, have robust default values, as illustrated by the fact that we have used the same values throughout all experiments in this article.

As illustrated in the numerical experiments, the approach does not successfully identify all parameters in all models. For time series, delay reconstructions are shown to be helpful, but still incur a loss of information compared to likelihood approaches. As a result, some parameters are only partially identified, such as  $(c, e)$  in the plankton model of Section 6.3. The choice of the lag parameter  $k$  would deserve further research, leveraging the vast literature on dynamical systems. Alternative methods to deal with dependent data would be helpful.

**Acknowledgements** We are grateful to Marco Cuturi and Guillaume Pouliot for helpful feedback on an earlier draft of this document.

## A Asymptotic properties of the MEWE

The MEWE of Section 2.3, defined as  $\hat{\theta}_{n,m} = \operatorname{arginf}_{\theta \in \mathcal{H}} \mathbb{E}[\mathfrak{W}_p(\hat{\mu}_n, \hat{\mu}_{\theta,m})]$ , where the expectation is taken with respect to the synthetic sample drawn from the model, can be shown to have similar properties as the MWE. On top of the assumptions of Section 4, we state the following extra condition.

**Assumption A.1.** *There exists a set  $E$  with  $\mathbb{P}(E) = 1$  such that, for all  $\omega \in E$ ,  $\sup_{\theta \in \mathcal{H}} |\mathbb{E}[\mathfrak{W}_p(\hat{\mu}_n(\omega), \hat{\mu}_{\theta,m})] - \mathfrak{W}_p(\hat{\mu}_n(\omega), \mu_\theta)| \rightarrow 0$  as  $m \rightarrow \infty$ .*

Assumption A.1 can be shown to hold if we assume that the model generates data such that one of the moment inequalities in Fournier and Guillin (2015) describing the rate of convergence of  $\mathbb{E}[\mathfrak{W}_p(\hat{\mu}_n, \hat{\mu}_{\theta,m})]$  to zero as  $m \rightarrow \infty$  holds, and the map  $\theta \mapsto M_q(\mu_\theta) = \int |x|^q d\mu_\theta(x)$  is bounded for some  $q > p$ , when  $\rho$  is assumed to be the Euclidean distance. We elaborate in the supplementary materials.

**Proposition A.1** (Existence of the MEWE). *Under Assumptions 4.2-4.5 and A.1, there exists a set  $E$  with  $\mathbb{P}(E) = 1$  such that for all  $\omega \in E$ , there exist  $n(\omega)$  and  $m(\omega)$  such that for all  $n \geq n(\omega)$  and  $m \geq m(\omega)$ , there exists  $\hat{\theta}_{n,m}(\omega)$  satisfying*

$$\hat{\theta}_{n,m}(\omega) \in \operatorname{arginf}_{\theta \in \mathcal{H}} \mathbb{E}[\mathfrak{W}_p(\hat{\mu}_n(\omega), \hat{\mu}_{\theta,m})].$$

**Proposition A.2** (Measurability of the MEWE). *Suppose that  $\mathcal{H}$  is a  $\sigma$ -compact Borel measurable subset of  $\mathbb{R}^{d_\theta}$ . Under Assumptions 4.1-4.5 and A.1, there exists a Borel measurable version of the MEWE.*

**Theorem A.1** (Consistency of the MEWE). *Under Assumptions 4.1-4.5 and A.1, any  $\hat{\theta}_{n,m}$  satisfying Proposition A.1 converges to  $\theta_*$ ,  $\mathbb{P}$ -almost surely as both  $n \rightarrow \infty$  and  $m \rightarrow \infty$ .*

No assumptions are put on the relationship between  $n$  and  $m$  in the above statements. In particular, the statements hold for  $\hat{\theta}_{n,n}$ , which can justify the use of the posterior mode as an approximation of the MWE

when  $n$  is large and the influence of the prior is small. Fixing  $n$ , the following proposition establishes a sense in which  $\hat{\theta}_{n,m}$  becomes close to  $\hat{\theta}_n$  as  $m \rightarrow \infty$ .

**Proposition A.3** (Limit of MEWE as  $m$  increases). *Suppose there exists a set  $E_0$  with  $\mathbb{P}(E_0) = 1$  such that, for all  $\omega \in E_0$ , there exist  $m(\omega)$  and  $\varepsilon_0 > 0$  such that  $\{\theta \in \mathcal{H} : \mathbb{E}[\mathfrak{W}_p(\hat{\mu}_n(\omega), \hat{\mu}_{\theta,m})] \leq \varepsilon_0\}$  is bounded for all  $m \geq m(\omega)$ . Under Assumptions 4.2-4.5 and A.1,*

$$\limsup_{m \rightarrow \infty} \operatorname{argmin}_{\theta \in \mathcal{H}} \mathbb{E}[\mathfrak{W}_p(\hat{\mu}_n(\omega), \hat{\mu}_{\theta,m})] \subset \operatorname{argmin}_{\theta \in \mathcal{H}} \mathfrak{W}_p(\hat{\mu}_n(\omega), \mu_\theta),$$

for all  $\omega \in E$ , where  $E$  is a set with  $\mathbb{P}(E) = 1$ .

## References

Andrieu, C., Doucet, A., and Holenstein, R. (2010). Particle Markov chain Monte Carlo (with discussion). *Journal of the Royal Statistical Society: Series B*, 72(4):357–385. [15](#), [23](#)

Andrieu, C. and Roberts, G. (2009). The pseudo-marginal approach for efficient Monte Carlo computations. *Annals of Statistics*, 37(2):697–725. [18](#)

Barndorff-Nielsen, O. E. and Shephard, N. (2001). Non-Gaussian Ornstein-Uhlenbeck-based models and some of their uses in financial economics. *Journal of the Royal Statistical Society: Series B*, 63(2):167–241. [23](#)

Barndorff-Nielsen, O. E. and Shephard, N. (2002). Econometric analysis of realized volatility and its use in estimating stochastic volatility models. *Journal of the Royal Statistical Society: Series B*, 64(2):253–280. [24](#)

Bassetti, F., Bodini, A., and Regazzini, E. (2006). On minimum Kantorovich distance estimators. *Statistics & probability letters*, 76(12):1298–1302. [2](#), [4](#), [10](#), [24](#)

Bassetti, F. and Regazzini, E. (2006). Asymptotic properties and robustness of minimum dissimilarity estimators of location-scale parameters. *Theory of Probability and its Applications*, 50(2):171–186. [2](#), [5](#), [11](#), [13](#)

Basu, A., Shioya, H., and Park, C. (2011). *Statistical inference: the minimum distance approach*. CRC Press. [1](#), [3](#)

Beaumont, M., Zhang, W., and Balding, D. (2002). Approximate Bayesian computation in population genetics. *Genetics*, 162(4):2025. [1](#)

Berger, J. O. and Wolpert, R. L. (1988). *Chapter 3: The Likelihood Principle and Generalizations*, volume Volume 6 of *Lecture Notes–Monograph Series*, pages 19–64. Institute of Mathematical Statistics. [1](#)

Bickel, P. J. and Freedman, D. A. (1981). Some asymptotic theory for the bootstrap. *Annals of Statistics*, 9(6):1196–1217. [12](#)

Bonassi, F. V. and West, M. (2015). Sequential Monte Carlo with adaptive weights for approximate Bayesian computation. *Bayesian Analysis*, 10(1):171–187. [21](#), [22](#)

Bonassi, F. V., You, L., and West, M. (2011). Bayesian learning from marginal data in bionetwork models. *Statistical applications in genetics and molecular biology*, 10(1). [21](#), [22](#)

Burkard, R., Dell'Amico, M., and Martello, S. (2009). *Assignment Problems*. Society for Industrial and Applied Mathematics (SIAM). [15](#)

Chanda, K. C. (1974). Strong mixing properties of linear stochastic processes. *Journal of Applied Probability*, 11(2):401–408. [12](#)

Cheney, E. W. and Wulbert, D. E. (1969). The existence and unicity of best approximations. *Mathematica Scandinavica*, 24:113–140. [13](#)

Chopin, N., Jacob, P., and Papaspiliopoulos, O. (2013). SMC<sup>2</sup>: an efficient algorithm for sequential analysis of state space models. *Journal of the Royal Statistical Society: Series B*, 75(3):397–426. [15](#), [23](#), [24](#)

Cuturi, M. (2013). Sinkhorn distances: Lightspeed computation of optimal transport. In *Advances in Neural Information Processing Systems (NIPS)*, pages 2292–2300. [2](#), [15](#)

Cuturi, M. and Doucet, A. (2014). Fast computation of Wasserstein barycenters. In *Proceedings of the 31st International Conference on Machine Learning (ICML)*, pages 685–693. [2](#), [15](#)

Dede, S. (2009). An empirical central limit theorem in  $l^1$  for stationary sequences. *Stochastic Processes and their Applications*, 119:3494 – 3515. [12](#)

del Barrio, E., Giné, E., and Matrán, C. (1999). Central limit theorems for the Wasserstein distance between the empirical and the true distributions. *Annals of Probability*, pages 1009–1071. [12](#)

Del Moral, P., Doucet, A., and Jasra, A. (2012). An adaptive sequential Monte Carlo method for approximate Bayesian computation. *Statistics and Computing*, 22(5):1009–1020. [18](#), [19](#)

Deligiannidis, G., Doucet, A., and Pitt, M. K. (2015). The correlated pseudo-marginal method. *arXiv preprint arXiv:1511.04992*. [20](#)

Diggle, P. J. and Gratton, R. J. (1984). Monte Carlo methods of inference for implicit statistical models. *Journal of the Royal Statistical Society B*, 46:193–227. [1](#)

Fearnhead, P. and Prangle, D. (2012). Constructing summary statistics for approximate Bayesian computation: semi-automatic approximate Bayesian computation. *Journal of the Royal Statistical Society: Series B*, 74(3):419–474. [6](#), [20](#)

Filippi, S., Barnes, C. P., Cornebise, J., and Stumpf, M. P. (2013). On optimality of kernels for approximate Bayesian computation using sequential Monte Carlo. *Statistical applications in genetics and molecular biology*, 12(1):87–107. [18](#)

Forneron, J.-J. and Ng, S. (2015). The ABC of simulation estimation with auxiliary statistics. *arXiv preprint arXiv:1501.01265*. [1](#)

Fournier, N. and Guillin, A. (2015). On the rate of convergence in Wasserstein distance of the empirical measure. *Probability Theory and Related Fields*, 162:707–738. [14](#), [25](#)

Frazier, D. T., Martin, G. M., Robert, C. P., and Rousseau, J. (2016). Asymptotic properties of approximate Bayesian computation. *arXiv preprint arXiv:1607.06903*. 6, 11, 14, 25

Genevay, A., Cuturi, M., Peyré, G., and Bach, F. (2016). Stochastic optimization for large-scale optimal transport. In *Advances in Neural Information Processing Systems (NIPS)*, pages 3432–3440. 2, 15

Gerber, M. and Chopin, N. (2015a). Convergence of sequential quasi-Monte Carlo smoothing algorithms. *Bernoulli (to appear)*. 15

Gerber, M. and Chopin, N. (2015b). Sequential quasi-Monte Carlo. *Journal of the Royal Statistical Society: Series B*, 77(3):509–579. 2, 15

Gini, C. (1914). Sulla misura della concentrazione e della variabilitá dei caratteri. *Atti R. Ist. Veneto Sci. Lett. Arti LXXIII (II)*, pages 1203–1248. 4

Gouriéroux, C., Monfort, A., and Renault, E. (1993). Indirect inference. *Journal of Applied Econometrics*, 8:85–118. 1

Ionides, E. L., Nguyen, D., Atchadé, Y., Stoev, S., and King, A. A. (2015). Inference for dynamic and latent variable models via iterated, perturbed Bayes maps. *Proceedings of the National Academy of Sciences*, 112(3):719–724. 23

Jacob, P. E., Lindsten, F., and Schön, T. B. (2016). Coupling of particle filters. *arXiv preprint arXiv:1606.01156*. 20

Jones, E., Parslow, J., and Murray, L. (2010). A Bayesian approach to state and parameter estimation in a phytoplankton-zooplankton model. *Australian Meteorological and Oceanographic Journal*, 59:7–16. 23

Kantorovich, L. V. (1942). On the translocation of masses. *Dokl. Akad. Nauk SSSR*, 37(7-8):227–229. 4

Kantz, H. and Schreiber, T. (1997). *Nonlinear time series analysis*. Cambridge University Press. 8, 9

Le Cam, L. (1970). On the assumptions used to prove asymptotic normality of maximum likelihood estimators. *Annals of Mathematical Statistics*, 41:802–828. 13

Lee, A. (2012). On the choice of MCMC kernels for approximate Bayesian computation with SMC samplers. In *Proceedings of the 2012 Winter Simulation Conference*, pages 304–315. 18, 19

Lee, A. and Łatuszyński, K. (2014). Variance bounding and geometric ergodicity of Markov chain Monte Carlo kernels for approximate Bayesian computation. *Biometrika*, 101(3):655–671. 19

Marin, J.-M., Pudlo, P., Robert, C. P., and Ryder, R. J. (2012). Approximate Bayesian computational methods. *Statistics and Computing*, 22(6):1167–1180. 1

Marjoram, P., Molitor, J., Plagnol, V., and Tavaré, S. (2003). Markov chain Monte Carlo without likelihoods. *Proceedings of the National Academy of Sciences*, 100(26):15324–15328. 18, 19

McFadden, D. (1989). A method of simulated moments for estimation of discrete response models without numerical integration. *Econometrica*, 57(5):995–1026. 1

Mengersen, K. L., Pudlo, P., and Robert, C. P. (2013). Bayesian computation via empirical likelihood. *Proceedings of the National Academy of Sciences*, 110(4):1321–1326. 9, 20

Moeckel, R. and Murray, B. (1997). Measuring the distance between time series. *Physica D*, 102:187–194. [8](#)

Mohamed, S. and Lakshminarayanan, B. (2016). Learning in implicit generative models. *arXiv preprint arXiv:1610.03483*. [1](#)

Montavon, G., Müller, K.-R., and Cuturi, M. (2016). Wasserstein training of restricted Boltzmann machines. In *Advances in Neural Information Processing Systems*, pages 3711–3719. [2](#), [17](#)

Murray, I. and Graham, M. M. (2016). Pseudo-marginal slice sampling. In *Proceedings of the 19th International Conference on Artificial Intelligence and Statistics (AISTATS)*, pages 911–919. [20](#)

Murray, L. M., Lee, A., and Jacob, P. E. (2016). Parallel resampling in the particle filter. *Journal of Computational and Graphical Statistics*, 25(3):789–805. [19](#)

Muskulus, M. and Verduyn-Lunel, S. (2011). Wasserstein distances in the analysis of time series and dynamical systems. *Physica D*, 240:45–58. [8](#)

Neath, R. C. et al. (2013). On convergence properties of the Monte Carlo EM algorithm. In *Advances in Modern Statistical Theory and Applications: A Festschrift in Honor of Morris L. Eaton*, pages 43–62. Institute of Mathematical Statistics. [17](#)

Owen, A. B. (2001). *Empirical likelihood*. CRC press. [3](#)

Park, M., Jitkrittum, W., Sejdinovic, D., and Unit, G. (2016). K2-ABC: Approximate Bayesian computation with kernel embeddings. In *Proceedings of the 19th International Conference on Artificial Intelligence and Statistics (AISTATS)*, pages 398–407. [1](#), [6](#)

Parr, W. C. and Schucany, W. R. (1980). Minimum distance and robust estimation. *Journal of the American Statistical Association*, 75(371):616–624. [5](#)

Pflug, G. C. and Pichler, A. (2014). *Multistage Stochastic Optimization*. Springer. [6](#)

Pollard, D. (1980). The minimum distance method of testing. *Metrika*, 27:43–70. [12](#), [13](#)

Prangle, D., Everitt, R. G., and Kypraios, T. (2016). A rare event approach to high dimensional approximate Bayesian computation. *arXiv preprint arXiv:1611.02492*. [1](#), [20](#)

Rabin, J., Peyré, G., Delon, J., and Bernot, M. (2011). Wasserstein barycenter and its application to texture mixing. In *International Conference on Scale Space and Variational Methods in Computer Vision*, pages 435–446. Springer. [15](#)

Rubio, F. J., Johansen, A. M., et al. (2013). A simple approach to maximum intractable likelihood estimation. *Electronic Journal of Statistics*, 7:1632–1654. [6](#), [18](#)

Sagan, H. (1994). *Space-filling curves*. Springer-Verlag New York. [2](#)

Santambrogio, F. (2015). Optimal transport for applied mathematicians. *Progress in Nonlinear Differential Equations and their applications*, 87. [4](#)

Schretter, C., He, Z., Gerber, M., Chopin, N., and Niederreiter, H. (2016). Van der Corput and golden ratio sequences along the Hilbert space-filling curve. In *Monte Carlo and Quasi-Monte Carlo Methods*, pages 531–544. Springer. [15](#)

Silk, D., Filippi, S., and Stumpf, M. P. (2013). Optimizing threshold-schedules for sequential approximate Bayesian computation: applications to molecular systems. *Statistical applications in genetics and molecular biology*, 12(5):603–618. [19](#)

Stark, J., Broomhead, D. S., Davies, M. E., and Huke, J. (2003). Delay embeddings for forced system: II. Stochastic forcing. *Journal of Nonlinear Science*, 13(6):519–577. [8](#)

Takens, F. (1981). Detecting strange attractors in turbulence. In Rand, D. A. and Young, L. S., editors, *Dynamical Systems and Turbulence, Lecture Notes in Mathematics*, volume 898, pages 230–242. Springer. [8](#)

The CGAL Project (2016). *CGAL User and Reference Manual*. CGAL Editorial Board, 4.8 edition. [16](#)

Toni, T., Welch, D., Strelkowa, N., Ipsen, A., and Stumpf, M. (2009). Approximate Bayesian computation scheme for parameter inference and model selection in dynamical systems. *Journal of the Royal Society Interface*, 6(31):187. [18](#)

Villani, C. (2008). *Optimal transport, old and new*. Springer-Verlag New York. [4](#), [11](#)

Wasserstein, L. N. (1969). Markov processes over denumerable products of spaces, describing large systems of automata. *Problemy Peredachi Informatsii*, 5(3):64–72. [4](#)

Wei, G. C. and Tanner, M. A. (1990). A Monte Carlo implementation of the EM algorithm and the poor man’s data augmentation algorithms. *Journal of the American Statistical Association*, 85(411):699–704. [17](#)

Wellner, J. A. and van der Vaart, A. W. (1996). *Weak Convergence and Empirical Processes*. Springer-Verlag New York. [13](#)

Wolfowitz, J. (1957). The minimum distance method. *The Annals of Mathematical Statistics*, 28(1):75–88. [1](#), [3](#)

Wood, S. N. (2010). Statistical inference for noisy nonlinear ecological dynamic systems. *Nature*, 466(7310):1102–1104. [1](#), [6](#), [18](#)

Zuluaga, C. D., Valencia, E. A., Álvarez, M. A., and Orozco, Á. A. (2015). A Parzen-based distance between probability measures as an alternative of summary statistics in approximate Bayesian computation. In *International Conference on Image Analysis and Processing*, pages 50–61. Springer. [1](#), [6](#)